Hydrogen Bond Directed Cocrystallization and Molecular Recognition Properties of Acyclic Imides

Margaret C. Etter* and Susan M. Reutzel

Contribution from the Department of Chemistry, University of Minnesota, Minneapolis, Minnesota 55455. *Received September 28, 1990*

Abstract: The cocrystallization behavior of acyclic imides is studied as a way to map out the hydrogen bond directed molecular recognition properties of a class of small biochemically related molecules under conditions where there is no preorganized cavity controlling the recognition events. Cocrystallization of over 80 imide-guest pairs was examined by solution and solid-state cocrystallization methods. The crystal structures of nine host-guest pairs are reported. The hydrogen bond patterns of 16 other cocrystal pairs were characterized by noncrystallographic means. Common hydrogen bond patterns and hydrogen bond selectivity properties were analyzed and are presented in the form of a set of hydrogen bond rules. Diacetamide was found to be a versatile cocrystallizing agent, forming 10 different cocrystal pairs. Imides that have a cis-trans conformation in their homomeric forms retain that conformation in their cocrystal structures. Imides that have a trans-trans conformation in their homomeric structures do not usually form cocrystals. Three imide cocrystal hydrogen types were observed repeatedly, with the most common pattern involving cyclic imide dimers with pendant hydrogen-bonded guests or cyclic heteromeric patterns having bivalent contacts between the imide and guest species. Guest molecules that successfully formed cocrystals covered a wide range of chemical types, including phenols, acids, amides, phosphine oxides, pyridines, imidazoles, and ureas.

Introduction

The use of cocrystallization as a way to study the molecular recognition properties of a single host molecule or of a class of related host molecules has been demonstrated.[1-3] When a strong intermolecular interaction, such as a hydrogen bond, drives the self-assembly of host and guest molecules, the number, orientation, and type of hydrogen-bonding functional groups on these molecules can be varied as a way to manipulate their aggregation patterns. This approach is particularly useful, and particularly informative, when all or nearly all steric constraints to aggregation have been removed. In other words, these systems have no preorganized cavities for trapping guest molecules; nevertheless, host-guest selectivity and predictable aggregation patterns are observed. While the role of hydrogen bonds in contributing extra stabilization to host-guest pairs with preorganized host cavities or clefts has been well-documented,[4] the directing and selectivity properties of the hydrogen bonds themselves have been all but ignored in host-guest systems.[5] In homomeric systems, the importance of hydrogen bond motifs has long been recognized,[6,7] and hydrogen bond selectivity in multifunctional homomeric crystals has also been shown.[8,9]

In this paper, molecular complexes of imides are prepared, showing that hydrogen bond selectivity criteria can be applied to heteromeric as well as to homomeric systems. Common features of their hydrogen bond aggregate structures are formulated as a set of rules, intended to be used as synthetic guidelines for designing new aggregate structures. Chemical rationale for the observed hydrogen bond selectivity properties and for the observed cocrystal stoichiometries are discussed in relation to the molecular recognition properties of imides.

Experimental Section

General Methods. Melting points were determined on a Fischer-Johns apparatus and are uncorrected. Infrared spectra were recorded on a Nicolet 5DXB FTIR spectrometer from Nujol mulls and are reported (cm^{-1}). ^1H and ^{13}C NMR spectra were recorded on IBM NR200AF and Varian VXR-300 spectrometers, respectively, and chemical shifts are reported in parts per million (δ) from Me_4Si. ^{13}C and ^{31}P CP/MAS NMR spectra were recorded on an IBM NR100AF spectrometer operating at a carbon frequency of 25.178 MHz and a phosphorus frequency of 40.55 MHz and with a Doty solid-state probe. ^{13}C chemical shifts are reported (δ) relative to *p*-di-*tert*-butylbenzene (CH_3 δ 31.0). ^{31}P chemical shifts are reported (δ) relative to triphenylphosphine oxide (δ 27.9). Spectroscopic-grade solvents were used for all recrystallizations. Deuterated solvents were obtained from Aldrich Chemical Co. Diacetamide (**1**) and other imide guest compounds were purchased from Aldrich and used without purification.

* Alfred P. Sloan Fellow, 1989-1991.

***N*-Acetylbenzamide (2).** *N*-Acetylbenzamide was obtained from an acid-catalyzed condensation of benzamide and acetic anhydride.[9]

2α. Recrystallization from acetone gives colorless blocks: mp 117-119 °C (lit.[10] mp 117 °C); IR (Nujol) 3270, 1745, 1740, 1680, 1520, 1490, 1470, 1370, 1270, 1220, and 700 cm^{-1}; ^{13}C CP/MAS NMR (25 MHz) δ 24.3, 25.4, 127.1, 129.1, 132.3, 162.7, 170.1, and 176.5.

2β. Recrystallization from ethanol gives colorless plates: mp 118-120 °C; IR (Nujol) 3270, 1740, 1680, 1510, 1490, 1470, 1370, 1280, 1220, and 700 cm^{-1}; ^{13}C CP/MAS NMR (25 MHz) δ 22.7, 129.4, 133.8, 164.3, 168.5, and 174.5; ^1H NMR (200 MHz, $CDCl_3$) δ 2.60 (s, 3 H), 7.48-7.61 (m, 3 H, *J* values include 7.1 and 1.8 Hz), 7.81 (dd, 2 H, *J* = 6.8 and 1.7 Hz), and 8.4 (b s, 1 H); ^{13}C NMR (75 MHz, $CDCl_3$) δ 25.6, 127.8, 128.8, 132.5, 133.1, 165.5, and 173.1.

***N*-Propionylbenzamide (3).** To a stirred solution of 5.0 g (41 mmol) of benzamide in 20 mL of acetonitrile was added dropwise 3.6 mL (41 mmol) of propionyl chloride in 5 mL of acetonitrile over 30 min. After the solution was refluxed for 6 h, it was poured over 100 mL of ice and warmed to room temperature. The product was filtered, washed, and recrystallized from diethyl ether to give **3** (2.5 g, 34%) as a white, crystalline solid: mp 95-98 °C (lit.[11] mp 98 °C); IR (Nujol) 3290, 1710,

(1) Etter, M. C.; Baures, P. W. *J. Am. Chem. Soc.* **1988**, *110*, 639-640.
(2) Etter, M. C.; Urbańczyk-Lipkowska, Z.; Zia-Ebrahimi, M.; Panunto, T. W. *J. Am. Chem. Soc.* **1990**, *112*, 8415-8426.
(3) Etter, M. C.; Adsmond, D. A. *J. Chem. Soc., Chem. Commun.* **1990**, *8*, 589-591.
(4) (a) Rebek, J., Jr.; Askew, B.; Ballester, P.; Costero, A. *J. Am. Chem. Soc.* **1988**, *110*, 923-927. (b) Rebek, J., Jr.; Askew, B.; Ballester, P.; Buhr, C.; Jones, S.; Nemeth, D.; Williams, K. *J. Am. Chem. Soc.* **1987**, *109*, 5033-5035. (c) Rebek, J., Jr. *Pure Appl. Chem.* **1989**, *61*, 1517-1522. (d) Askew, B.; Ballester, P.; Buhr, C.; Jeong, K. S.; Jones, S.; Parris, K.; Williams, K.; Rebek, J., Jr. *J. Am. Chem. Soc.* **1989**, *111*, 1082-1090. (e) Rebek, J., Jr.; Askew, B.; Islam, N.; Killoran, M.; Nemeth, D.; Wolak, R. *J. Am. Chem. Soc.* **1985**, *107*, 6736-6738. (f) Rebek, J., Jr.; Nemeth, D. *J. Am. Chem. Soc.* **1985**, *107*, 6738-6739. (g) Rebek, J., Jr. *Science* **1987**, *235*, 1478-1484. (h) Zimmerman, S. C.; Wu, W. *J. Am. Chem. Soc.* **1989**, *111*, 8054-8055. (i) Chang, S.-K.; Hamilton, A. D. *J. Am. Chem. Soc.* **1988**, *110*, 1318-1319. (j) Kelly, T. R.; Maguire, M. P. *J. Am. Chem. Soc.* **1987**, *109*, 6549-6551. (k) Bell, T. W.; Liu, J. *J. Am. Chem. Soc.* **1988**, *110*, 3673-3674. (l) Sheridan, R. E.; Whitlock, H. W., Jr. *J. Am. Chem. Soc.* **1986**, *108*, 7120-7121.
(5) (a) Weber, E.; Csöregh, I.; Stensland, B.; Czugler, M. *J. Am. Chem. Soc.* **1984**, *106*, 3297-3306. (b) Weber, E.; Hecker, M.; Csöregh, I.; Czugler, M. *J. Am. Chem. Soc.* **1989**, *111*, 7866-7872. (c) Toda, F. *Top. Curr. Chem.* **1987**, *140*, 43-69. (d) Hart, H.; Lin, L.-T. W.; Ward, D. L. *J. Am. Chem. Soc.* **1984**, *106*, 4043-4045. (e) Hart, H.; Lin, L.-T. W.; Goldberg, I. *Mol. Cryst. Liq. Cryst.* **1986**, *137*, 277-286. (f) Goldberg, I.; Lin, L.-T. W.; Hart, H. *J. Inclus. Phenom.* **1984**, *2*, 377-389. (g) Seto, C. T.; Whitesides, G. M. *J. Am. Chem. Soc.*, in press.
(6) Leiserowitz, L.; Schmidt, G. M. J. *J. Chem. Soc. A* **1969**, 2372-2382.
(7) (a) Leiserowitz, L. *Acta Crystallogr.* **1976**, *B32*, 775-802. (b) Leiserowitz, L.; Tuval, M. *Acta Crystallogr.* **1978**, *B34*, 1230-1247.
(8) Etter, M. C. *Acc. Chem. Res.* **1990**, *23*, 120-126.
(9) Baburao, K.; Costello, A. M.; Petterson, R. C.; Sander, G. E. *J. Chem. Soc. C* **1968**, 2779-2781.
(10) Tóth, G. *Acta Chim. Acad. Sci. Hung.* **1970**, *1*, 101-109.
(11) Dunn, P.; Parkes, E. A.; Polya, J. B. *Rec. Trav. Chim.* **1952**, *71*, 676-683.

0002-7863/91/1513-2586$02.50/0

1680, 1500, 1470, 1370, 1240, 1210, 1080, and 710 cm^{-1}; ^1H NMR (200 MHz, $CDCl_3$) δ 1.22 (t, 3 H, J = 7.3 Hz), 3.03 (q, 2 H, J = 7.3 Hz), 7.46–7.61 (m, 3 H, J values include 7.2 Hz), 7.84 (dd, 2 H, J = 7.0 Hz), and 8.61 (b s, 1 H); ^{13}C NMR (75 MHz, $CDCl_3$) δ 31.1, 127.9, 128.6, 132.6, 132.9, 165.4, and 176.7; ^{13}C CP/MAS NMR (25 MHz) δ 7.3, 31.8, 128.8, 131.0, 162.9, 170.0, 175.8, and 183.6.

***N*-Butyrylbenzamide (4).** To a stirred solution of 5.0 g (41 mmol) of benzamide in 20 mL of acetonitrile was added dropwise 4.3 mL (41 mmol) of *n*-butyryl chloride over 30 min. After the solution was refluxed for 3 h, it was poured over 100 mL of ice and warmed to room temperature. The product was filtered, washed, and recrystallized from toluene to give **4** (3.5 g, 44%) as a white crystalline solid: mp 103–104 °C (lit.[11] mp 104 °C); IR (Nujol) 3290, 1710, 1680, 1670, 1600, 1580, 1510, 1470, 1380, 1320, 1240, and 1190 cm^{-1}; ^1H NMR (200 MHz, $CDCl_3$) δ 1.03 (t, 3 H, J = 7.4 Hz), 1.74 (sext, 2 H, J = 7.4 Hz), 2.99 (t, 2 H, J = 7.4 Hz), 7.50–7.65 (m, 3 H, J = 1.5, 7.5, 7.6, and 7.0 Hz), 7.85 (dd, 2 H, J = 6.9 and 1.6 Hz), and 8.7 (b s, 1 H); ^{13}C NMR (50 MHz, $CDCl_3$) δ 13.7, 17.6, 39.6, 128.1, 128.8, 133.0, 166.0, and 177.2; ^{13}C CP/MAS NMR (25 MHz) δ 12.4, 14.2, 40.3, 127.4, 130.1, 133.8, 161.0, 167.9, 175.3, and 182.1.

Dibenzamide (5). Dibenzamide was obtained from a base-catalyzed condensation of benzamide and benzoyl chloride.[12] Recrystallization from diethyl ether gives colorless needles: mp 144–145 °C (lit.[12] mp 144 °C); IR (Nujol) 3240, 1700, 1500, 1230, and 710 cm^{-1}; ^1H NMR (200 MHz, $CDCl_3$) δ 7.44–7.62 (m, 6 H, J = 7.5 Hz), 7.86 (dd, 4 H, J = 6.9 and 1.6 Hz), and 9.0 (b s, 1 H); ^{13}C NMR (75 MHz, $CDCl_3$) δ 127.9, 128.9, 133.1, 133.3, and 166.2; ^{13}C CP/MAS NMR (25 MHz) δ 129.7, 132.5, 134.4, 168.0, and 174.

Other Imides. Six other imides, dipropionamide (**6**), *N*-acetylpropionamide (**7**), diisobutyramide (**8**), *N*-(cyclohexylcarbonyl)cyclohexylamide (**9**), *N*-(phenylacetyl)phenylacetamide (**10**), and *N*-isobutyrylbenzamide (**11**), were synthesized. Details of their syntheses and product analyses are available in the supplementary material.

General Methods for the Preparation of Imide Cocrystals. Imide cocrystals can be obtained by solution, solid-state, or melt techniques.

Method A (solution): Equimolar amounts of the imides and guest molecules are dissolved in a mutually miscible solvent(s) and are allowed to recrystallize slowly at room temperature. When possible, the crystals are removed from solution as soon as they are formed and before the solvent has completely evaporated. Alternately, cocrystals are obtained after all of the solvent(s) has evaporated.

Method B (solid state): Equimolar amounts of the imides and guest molecules are ground together in a Wig-L-Bug dental amalgamator for 10 min. Conversion of the starting materials to the cocrystal in the solid state approaches 100%.

Method C (melt): Equimolar amounts of the imides and guest molecules are melted together and cooled to room temperature.

Cocrystals prepared by all methods were characterized by physical and spectroscopic methods. In all cases where two or more methods were used for one system, the same solid-state phases were obtained from the different methods.

Diacetamide (1)–4-nitrophenol (1:1) cocrystal (12): methods A and B; colorless, irregular (1:1 toluene–$CHCl_3$); mp 75–77 °C; IR (Nujol) 3160, 1720, 1680, 1590, 1510, 1500, 1460, 1370, 1330, 1290, 1270, 1240, 1170, 1110, 1030, 860, 750, 650, and 630 cm^{-1}; ^1H NMR (200 MHz, $CDCl_3$) δ 2.32 (s, 6 H), 6.34 (b s, 1 H), 6.91 (dd, 2 H, J = 9.1 and 2.1 Hz), 8.16 (dd, 2 H, 9.1 and 2.2 Hz), and 8.2 (b s, 1 H); ^{13}C CP/MAS NMR (25 MHz) δ 25.6, 115.4, 126.2, 137.6, 141.7, 163.6, 173.5, and 177.

***N*-Butyrylbenzamide (4)–4-nitrophenol (1:1) cocrystal (13):** methods A and B; colorless prisms (toluene); mp 94–95 °C; IR (Nujol) 3290, 3250, 1710, 1670, 1600, 1520, 1500, 1470, 1340, 1310, 1280, 1260, 1230, 1180, 1160, 1110, and 710 cm^{-1}; ^1H NMR (200 MHz, $(CD_3)_2CO$) δ 0.97 (t, 3 H, J = 7.3 Hz), 1.68 (sext, 2 H, J = 7.3 and 7.4 Hz), 2.84 (t, 2 H, J = 7.3 Hz), 7.02 (d, 2 H, J = 9.2 Hz), 7.49–7.64 (m, 3 H, J = 7.6, 1.6, 7.2, and 7.0 Hz), 7.99 (dd, 2 H, J = 6.9 and 1.6 Hz), 8.16 (dd, 2 H, J = 9.1 Hz), and 9.9 (b s, 1 H); ^{13}C CP/MAS NMR (25 MHz) δ 12.5, 15.9, 41.0, 115.4, 128.1, 135.1, 141.7, 162.0, 169.9, 175.2, and 182.7.

Diacetamide (1)–hydroquinone (2:1) cocrystal (14): methods A and B; colorless plates (1:1 toluene–ethanol); mp 77–79 °C; IR (Nujol) 3450, 3270, 3250, 3210, 3180, 1730, 1690, 1520, 1510, 1470, 1370, 1300, 1250, 1230, 1200, 1030, 840, and 760 cm^{-1}; ^1H NMR (200 MHz, $(CD_3)_2CO$) δ 2.20 (s, 12 H), 6.66 (s, 4 H), 7.67 (s, 2 H), and 9.6 (b s, 1 H); ^{13}C CP/MAS NMR (25 MHz) δ 25.0, 114.9, 149.4, 168.2, 174.5, and 181.6.

***N*-Butyrylbenzamide (4)–hydroquinone (2:1) cocrystal (15):** methods A and B; colorless plates (1:1 toluene–acetone); mp 120–121 °C; IR (Nujol) 3370, 3290, 1700, 1670, 1520, 1470, 1310, 1250, 1210, 1190, and 700 cm^{-1}; ^1H NMR (200 MHz, $(CD_3)_2CO$) δ 0.97 (t, 6 H, J = 7.4 Hz), 1.68 (sext, 4 H, J = 7.3 and 7.3 Hz), 2.84 (t, 4 H, J = 7.3 Hz), 6.66 (s, 4 H), 7.48–7.67 (m, 8 H, J = 7.4 and 1.6 Hz), 7.99 (dd, 4 H, J = 7.0 and 1.4 Hz), and 9.9 (b s, 2 H); ^{13}C CP/MAS NMR (25 MHz) δ 12.7, 16.1, 40.4, 115.0, 116.4, 128.9, 133.4, 150.0, 164.1, 171.1, 175.5, and 182.4.

Diacetamide (1)–4-hydroxybenzoic acid (1:1) cocrystal (16): methods A and B; colorless blocks (ethyl acetate); mp 126–128 °C; IR (Nujol) 3140, 1770, 1720, 1680, 1650, 1610, 1590, 1300, 1290, 1250, 1230, 1160, and 1030 cm^{-1}; ^1H NMR (200 MHz, $(CD_3)_2CO$) δ 2.21 (s, 6 H), 6.92 (dd, 2 H, J = 8.9 and 2.0 Hz), 7.91 (dd, 2 H, J = 8.7 and 2.0 Hz), and 9.7 (b s, 1 H); ^{13}C CP/MAS NMR (25 MHz) δ 25.6, 116.0, 116.5, 120.0, 132.7, 162.0, 170.5, 174.5, and 179.4.

Diacetamide (1)–4-hydroxybenzamide (1:1) cocrystal (17): methods A and B; colorless prisms (acetonitrile); mp 124–127 °C; IR (Nujol) 3470, 3350, 3230, 3120, 1720, 1680, 1640, 1620, 1580, 1540, 1520, 1400, 1290, 1240, and 1030 cm^{-1}; ^1H NMR (200 MHz, $(CD_3)_2CO$) δ 2.20 (s, 3 H), 6.4 (b s, 1 H), 6.87 (dd, 2 H, J = 8.7 and 1.9 Hz), 7.3 (b s, 1 H), 7.83 (dd, 2 H, J = 8.7 and 1.9 Hz); ^{13}C CP/MAS NMR (25 MHz) δ 25.0, 114.9, 120.7, 129.6, 162.2, 167.7, and 173.7.

***N*-Acetylbenzamide (2)–triphenylphosphine oxide (1:1) cocrystal (18):** methods A and B; colorless prisms (1:1 toluene–acetone); mp 122–123 °C; IR (Nujol) 3090, 3050, 1710, 1690, 1670, 1510, 1480, 1460, 1440, 1370, 1280, 1260, 1190, 1180, 1120, 1070, 1020, 720, 710, 700, 690, and 680 cm^{-1}; ^1H NMR (200 MHz, $(CD_3)_2CO$) δ 2.45 (s, 3 H), 7.52–7.75 (m, 18 H), 8.00 (dd, 2 H, J = 6.8 and 1.7 Hz), and 10.0 (b s, 1 H); ^{13}C CP/MAS NMR (25 MHz) δ 25.3, 127.8, 132.6, 165.2, 171.8, and 178.4; ^{31}P CP/MAS NMR (40 MHz) δ 29.8.

***N*-Propionylbenzamide (3)–triphenylphosphine oxide (1:1) cocrystal (19):** methods A and B; colorless prisms (1:1 toluene–acetone); mp 103–105 °C; IR (Nujol) 3093, 3058, 1710, 1683, 1460, 1436, 1369, 1259, 1202, 1188, 1120, 722, 707, and 695 cm^{-1}; ^1H NMR (200 MHz, $(CD_3)_2CO$) δ 1.12 (t, 3 H, J = 7.4 Hz), 2.88 (q, 2 H, J = 7.4 Hz), 7.53–7.75 (m, 18 H), 8.00 (d, 2 H, J = 6.9 Hz), and 9.9 (b s, 1 H); ^{13}C CP/MAS NMR (25 MHz) δ 10.5, 31.6, 127.5, 131.4, 164.4, 170.6, 175.3, and 182.3; ^{31}P CP/MAS NMR (40 MHz) δ 35.8.

Dibenzamide (5)–triphenylphosphine oxide (1:1) cocrystal (20): methods A and B; colorless prisms (1:1 toluene–acetone); mp 120–122 °C; IR (Nujol) 3210, 3140, 3060, 1730, 1510, 1480, 1470, 1440, 1230, 1180, 1120, 710, and 700 cm^{-1}; ^1H NMR (200 MHz, $(CD_3)_2CO$) δ 7.48–7.73 (m, 21 H), 7.99 (dd, 4 H, J = 7.0 and 1.1 Hz), and 10.4 (b s, 1 H); ^{13}C CP/MAS NMR (25 MHz) δ 128.7, 132.4, 162.9, 166.8, 170.6, and 173.0; ^{31}P CP/MAS NMR (40 MHz) δ 26.0.

***N*-Propionylbenzamide (3)–4-nitrophenol (1:1) cocrystal (21):** methods A and B; colorless rods (1:1 ethanol–toluene); mp 85–87 °C; IR (Nujol) 3240, 3160, 1710, 1680, 1620, 1600, 1500, 1490, 1460, 1340, 1290, 1270, 1240, 1210, 1110, and 710 cm^{-1}; ^1H NMR (200 MHz, $(CD_3)_2CO$) δ 1.12 (t, 3 H, J = 7.4 Hz), 2.90 (q, 2 H, J = 7.4 Hz), 7.02 (d, 2 H, 9.2 Hz), 7.48–7.67 (m, 3 H, J values include 8.1 Hz), 8.00 (d, 2 H, J = 8.4 and 6.8 Hz), 8.16 (d, 2 H, J = 9.2 Hz), and 9.9 (b s, 1 H); ^{13}C CP/MAS NMR (25 MHz) δ 7.5, 32.2, 114.8, 139.5, 162.2, 167.4, 176.9, and 183.4.

Diacetamide (1)–4-cyanophenol (1:1) cocrystal (22): methods A and C; colorless blocks (1:1 toluene–acetone); mp 53–54 °C; IR (Nujol) 3160, 2220, 1680, 1660, 1610, 1590, 1510, 1490, 1280, 1250, 1170, 1030, 840, and 700 cm^{-1}; ^1H NMR (200 MHz, $(CD_3)_2CO$) δ 2.21 (s, 6 H), 2.53 (b s, 1 H), 7.00 (dd, 2 H, J = 2.0 and 8.7 Hz), 7.61 (dd, 2 H, J = 2.0 and 8.9 Hz), and 9.5 (b s, 1 H); ^{13}C CP/MAS NMR (25 MHz) δ 25.4, 98.3, 114.3, 134.3, 134.8, 160.6, and 173.5.

***N*-Butyrylbenzamide (4)–4-bromophenol (1:1) cocrystal (23):** methods A and B; colorless needles (1:1 toluene–acetone); mp 75–76 °C; IR (Nujol) 3350, 3300, 1700, 1680, 1670, 1590, 1490, 1470, 1430, 1310, 1250, 1220, 1190, 830, and 700 cm^{-1}; ^1H NMR (200 MHz, $(CD_3)_2CO$) δ 0.97 (t, 3 H, J = 7.4 Hz), 1.68 (sext, 2 H, J = 7.4 Hz), 2.84 (t, 2 H, J = 7.3 Hz), 6.80 (dd, 2 H, J = 9.0 and 2.3 Hz), 7.33 (dd, 2 H, J = 9.0 and 2.3 Hz), 7.48–7.63 (m, 3 H, J values include 7.1 Hz), 7.99 (d, 2 H, J = 7.0 Hz), 8.61 (b s, 1 H), and 9.9 (b s, 1 H); ^{13}C CP/MAS NMR (25 MHz) δ 13.6, 41.2, 117.8, 129.2, 157.0, 164.5, 171.0, 175.4, and 182.7.

***N*-Propionylbenzamide (3)–4-bromophenol (1:1) cocrystal (24):** methods A and B; colorless prisms (1:1 toluene–acetone); mp 52–53 °C; IR (Nujol) 3290, 1700, 1680, 1590, 1510, 1490, 1470, 1430, 1370, 1270, 1260, 1200, 1070, 810, and 710 cm^{-1}; ^1H NMR (200 MHz) δ 1.12 (t, 3 H, J = 7.3 Hz), 2.88 (q, 2 H, J = 7.3 Hz), 6.80 (dd, 2 H, J = 8.8 and 2.1 Hz), 7.33 (dd, 2 H, J = 8.8 and 2.1 Hz), 7.49–7.64 (m, 3 H, J values include 7.5, 7.0, and 1.6 Hz), 7.99 (dd, 2 H, J = 7.0 and 1.7 Hz), 8.6 (b s, 1 H), and 9.9 (b s, 1 H); ^{13}C CP/MAS NMR (25 MHz) δ 7.6, 31.0, 117.2, 131.0, 155.3, 165.2, 171.8, 176.8, and 182.7.

***N*-Butyrylbenzamide (4)–4-chlorophenol (1:1) cocrystal (25):** methods A and B; colorless needles (1:1 toluene–acetone); mp 64–67 °C; IR

(12) (a) Titherley, A. W. *J. Chem. Soc.* **1904**, *85*, 1673–1691. (b) Mizrahi, V.; Niven, M. L. *S. Afr. J. Chem.* **1983**, *36* (4), 137–142.

Table I. Summary of Imide–Guest Cocrystallization Experiments

Imide–Guest Pairs That Form Cocrystals

imide	guests	imide	guests
diacetamide (**1**)	b, g, j, k, m, q, s, u, v, hh	*N*-propionylbenzamide (**3**)	b, e, m, kk
diacetamide (**1**)[a]	a, e, f, y, bb–dd	*N*-butyrylbenzamide (**4**)	b, e, f, m
N-acetylbenzamide (**2**)	kk	dibenzamide (**5**)	kk

Imide–Guest Pairs That Do Not Form Cocrystals

imide	guests	imide	guests
diacetamide (**1**)	c, d, h, l, o, p, r, t, w, z, aa, ee–gg, ii–kk	dipropionamide (**6**)	k, m
N-acetylbenzamide (**2**)	b, k, m, w, x, cc	*N*-acetylpropionamide (**7**)	kk
N-propionylbenzamide (**3**)	gg, i–l, q, y, bb, cc	diisobutyramide (**8**)	kk
N-butyrylbenzamide (**4**)	g, i–l, q, y, hh, kk	*N*-(cyclohexylcarbonyl)cyclohexylamide (**9**)	kk
dibenzamide (**5**)	b, k, n, u, hh	*N*-(phenylacetyl)phenylacetamide (**10**)	kk
		N-isobutyrylbenzamide (**11**)	kk

Codes for Guest Molecules

a	phenol	n	perfluorophenol	z	2-amino-5-bromopyridine
b	hydroquinone	o	benzoic acid	aa	2-amino-5-nitropyridine
c	4-acetamidophenol	p	4-aminobenzoic acid	bb	2-aminopyridine
d	4-aminophenol	q	3,4-dinitrobenzoic acid	cc	imidazole
e	4-bromophenol	r	3,5-dinitrobenzoic acid	dd	4-methylimidazole
f	4-chlorophenol	s	4-(methylamino)benzoic acid	ee	4-nitroimidazole
g	4-cyanophenol	t	4-nitrobenzoic acid	ff	4-phenylimidazole
h	2,4-dinitrophenol	u	acetamide	gg	carbanilide
i	4-hydroxyacetophenone	v	benzamide	hh	1,3-dimethylurea
j	4-hydroxybenzamide	w	*N*-methylbenzamide	ii	adenine
k	4-hydroxybenzoic acid	x	*N*-phenylacetamide	jj	*N*-methyl-4-nitroaniline
l	methyl 4-hydroxybenzoate	y	2-hydroxypyridine	kk	triphenylphosphine oxide
m	4-nitrophenol				

[a] These host–guest pairs form cocrystals that are liquids at room temperature.

(Nujol) 3360, 3240, 3160, 1710, 1670, 1600, 1590, 1490, 1470, 1430, 1350, 1310, 1260, 1250, 1220, 1160, 1090, 830, 720, and 640 cm^{-1}; ^1H NMR (200 MHz, $(CD_3)_2CO$) δ 0.98 (t, 3 H, J = 7.3 Hz), 1.67 (sext, 2 H, J = 7.3 Hz), 2.85 (t, 2 H, J = 7.2 Hz), 6.84 (dd, 2 H, J = 2.3 and 6.6 Hz), 7.19 (dd, 2 H, J = 2.2 and 6.7 Hz), 7.49–7.67 (m, 3 H, J = 7.5, 7.0, and 1.5 Hz), and 7.99 (dd, 2 H, J = 1.6 and 7.0 Hz); ^{13}C CP/MAS NMR (25 MHz) δ 16.1, 40.9, 119.8, 128.8, 155.0, 164.3, 174.5, and 179.9.

***N*-Propionylbenzamide (3)–hydroquinone (2:1) cocrystal (26)**: methods A and B; colorless plates (1:1 toluene–ethyl acetate); mp 104–106 °C; IR (Nujol) 3430, 3290, 1700, 1680, 1520, 1460, 1370, 1250, 1210, 1200, 1190, 1080, 900, 820, 760, and 710 cm^{-1}; ^1H NMR (200 MHz, $(CD_3)_2CO$) δ 1.12 (t, 6 H, J = 7.4 Hz), 2.88 (q, 4 H, J = 7.3 Hz), 6.66 (s, 4 H), 7.49–7.67 (m, 8 H, J = 2.0 and 7.0 Hz), 7.99 (dd, 4 H, J = 2.0 and 6.8 Hz), and 9.8 (b s, 2 H); ^{13}C CP/MAS NMR (25 MHz) δ 5.5, 30.3, 113.6, 128.3, 132.4, 148.4, 161.6, 168.1, 175.8, and 182.9.

Diacetamide (1)–acetamide (1:1) cocrystal (27): method B; mp 59–62 °C; IR (Nujol) 3300, 3240, 3120, 1730, 1690, 1660, 1630, 1530, 1380, 1290, 1240, 1130, and 1040 cm^{-1}; ^{13}C CP/MAS NMR (25 MHz) δ 20.9, 23.6, 26.0, 170.6, 174.9, and 180.2.

Diacetamide (1)–benzamide (1:1) cocrystal (28): method B; mp 64–67 °C; IR (Nujol) 3460, 3350, 3280, 3240, 3130, 1740, 1680, 1640, 1610, 1570, 1530, 1460, 1450, 1410, 1380, 1290, 1250, 1220, 1020, and 720 cm^{-1}; ^{13}C CP/MAS NMR (25 MHz) δ 24.2, 128.3, 131.6, 169.9, 174.7, and 180.3.

Diacetamide (1)–4-(methylamino)benzoic acid (1:1) cocrystal (29): methods A and B; yellow rods (ethyl acetate); mp 132–134 °C; IR (Nujol) 3400, 3370, 3150, 2660, 2540, 1700, 1660, 1600, 1540, 1520, 1510, 1420, 1320, 1290, 1280, 1230, and 1180 cm^{-1}; ^1H NMR (200 MHz, $(CD_3)_2CO$) δ 2.20 (s, 6 H), 5.8 (b s, 2 H), 6.62 (dd, 2 H, J = 8.9 and 1.9 Hz), and 7.81 (dd, 2 H, J = 8.9 and 2.0 Hz); ^{13}C CP/MAS NMR (25 MHz) δ 24.3, 34.7, 106.9, 108.5, 114.0, 130.9, 133.3, 151.1, 160.6, 168.7, 172.8, and 179.2.

Diacetamide (1)–3,4-dinitrobenzoic acid (1:1) cocrystal (30): method B; mp 74–78 °C; IR (Nujol) 3300, 3250, 3200, 3150, 3120, 1740, 1720, 1560, 1530, 1390, 1370, 1350, 1260, 1210, 1150, and 1110 cm^{-1}; ^1H NMR (200 MHz, $(CD_3)_2CO$) δ 2.20 (s, 6 H), 8.32 (d, 1 H, J = 8.2 Hz), 8.58 (dd, 1 H, J = 9.9 and 2 Hz), 8.67 (d, 1 H, J = 1.5 Hz), and 9.6 (b s, 1 H); ^{13}C CP/MAS NMR (25 MHz) δ 25.1, 124.8, 128.9, 133.3, 138.8, 139.3, 144.6, 147.3, 163.3, 171.2, 172.6, 178.0, and 179.2.

Diacetamide (1)–1,3-dimethylurea (1:1) cocrystal (31): methods A, B, and C; colorless flakes ($CHCl_3$); mp 55–58 °C; IR (Nujol) 3400, 3360, 3250, 3170, 1760, 1660, 1610, 1570, 1530, 1500, 1460, 1380, 1370, 1270, 1190, and 1170 cm^{-1}; ^1H NMR (200 MHz, $CDCl_3$) δ 2.30 (s, 6 H), 2.77 (d, 6 H, J = 4.9 Hz), 4.43 (b s, 2 H), and 8.6 (b s, 1 H); ^{13}C CP/MAS NMR (25 MHz) δ 24.6, 32.5, 153.9, 163.4, 169.4, and 175.6.

Imide Cocrystals That Are Neat Liquids at Room Temperature. Seven 1:1 cocrystals of diacetamide and other organic guest donors and acceptors that melt below room temperature have been prepared as described previously. These host–guest pairs are indicated in Table I.

The formation of hydrogen bonded heteromers in the neat liquids was confirmed by the presence of new peaks in their IR spectra. The occurrence of melting points of the host–guest pairs at 10–80 °C below that of either of the components or below room temperature was used as supporting evidence for cocrystal formation, although in some cases lowered melting points may simply be due to eutectic formation. The structures of the hydrogen bonded aggregates in the neat liquids were not explored in detail.

Imide–Guest Pairs That Do Not Form Cocrystals. Many attempts at cocrystallizing imides with a variety of hydrogen bond donor and acceptor guests were not successful by either solution or solid-state methods. The imide–guest pairs that did not form cocrystals are shown in Table I. Spectroscopic and physical methods were used to show that separate phases of each component were present in the solid-state products of these imide–guest mixtures.

Crystallographic Literature Search. A Cambridge Crystallographic Data Base Search (Version 4.3) for acyclic imides and their complexes was carried out.[13] From the connectivity search of C–CO–NH–CO–C, 23 structures were obtained. Of these, 13 were uncomplexed imides, 9 were imide cocrystals with group I or II metal halides, and 1 was an imide cocrystal with an organic guest. The search algorithm and bibliographic citations retrieved from the search are included in the supplementary material.

Crystal Structure Determinations for Compounds 12–20. Data were collected on an Enraf-Nonius CAD4 diffractometer with graphite monochromated Mo Kα radiation (λ = 0.71069) using the ω–2θ scan technique. Lattice parameters were obtained from least-squares analysis of 25 reflections. Structures were solved by direct methods with MITHRIL[14] and DIRDIF.[15] All non-hydrogen atoms were refined anisotropically. All NH and OH protons were refined isotropically. The acetyl hydrogen atoms were refined isotropically as a group. The other hydrogen atoms included in the structure factor calculations were placed in idealized positions (d_{C-H} = 0.95 Å) with assigned isotropic thermal parameters (B = 1.2B of bonded atoms). The experimental details for the X-ray analysis of nine imide cocrystals are listed in Table II. The

(13) *Cambridge Structural Database*; Cambridge Crystallographic Data Centre, University Chemical Laboratoty: Cambridge, England, June 1990 update; Version 4.3 (Vax).

(14) Gilmore, C. J. *J. Appl. Crystallogr.* **1984**, *17*, 42–46.

(15) Beurskens, P. T. Technical Report, University of Nijmegen: The Netherlands, 1984; Vol. 1.

last line in the table gives the graph set for each structure. The graph set is a representation of the topology of hydrogen-bonded sets of molecules in the crystal.[16] Descriptions of how these assignments were made and of how to use graph sets to analyze acyclic imide patterns will be given in a future paper.

Results

The cocrystallization of acyclic imides with hydrogen bond donor and acceptor guest molecules was explored to test solid-state selectivity preferences of hydrogen-bonding groups. As we have done with ureas and nitroanilines previously, we wanted to see if a set of hydrogen bond rules useful for designing new imide aggregate structures could be developed. When cocrystal pairs were designed, intramolecular hydrogen bonding interactions that would compete with intermolecular hydrogen bonding were avoided by using imides that had no competitive hydrogen bonding functional groups, besides CO–NH–CO, and by using guest molecules with no near-neighbor hydrogen bond donor and acceptor groups. Over 80 host–guest pairs were evaluated, including 11 aromatic and/or aliphatic acyclic imides, and a variety of hydrogen bond guest molecules was attempted. Cocrystalline solids formed for 25 of these host–guest pairs. Successful guest molecules included phenols, carboxylic acids, amides, phosphine oxides, and ureas. The crystal structures of single crystals of nine imide cocrystals are presented. The hydrogen bond patterns of homomeric imide crystals and of their heteromeric cocrystals are compared geometrically and topologically.

Crystallographic Studies of Acyclic Imides. Acyclic imides have three planar conformations, cis–cis (cc), cis–trans (ct), and trans–trans (tt), differentiated by the relative orientations of the carbonyl groups to the central NH bond. The cc conformer has

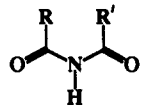

cis-cis (cc)

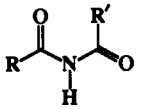

cis-trans (ct)

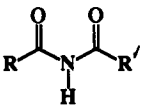

trans-trans (tt)

the highest energy due to steric overcrowding between R and R′. This conformer has not been observed in solution or in the solid state for any known acyclic imides. The ct conformer is the most stable form and is observed in solution for all simple acyclic imides (11 examples) except dipivalamide.[17] The tt conformer is destabilized by ~4 kJ/mol relative to the ct conformer by the electrostatic repulsion between the two imide carbonyl groups; nevertheless, it is frequently observed in the solid state.[18]

Diacetamide (**1**), the simplest of the acyclic imides, crystallizes in two polymorphic forms: α, the stable form, containing molecules with the ct conformation, and β, the metastable form containing molecules with the tt conformation.[19,20] When **1** is complexed

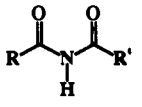

	R	R′	conformer in crystals		R	R′	conformer in crystals
1α,β	Me	Me	ct, tt	**7**	Me	Et	tt
2α,β	Me	Ph	ct, tt	**8**	*i*-Pr	*i*-Pr	tt
3	Et	Ph	ct	**9**	Cy	Cy	tt
4	Pr	Ph	ct	**10**	Bn	Bn	tt
5	Ph	Ph	tt	**11**	*i*-Pr	Ph	tt
6	Et	Et	tt				

with organic molecules, the ct conformation is retained. The only conditions under which **1** forms its tt conformer in a cocrystal are when it is complexed with group I or II metal halides.[21] Three other examples of simple, acyclic imides, *N*-acetylbenzamide (**2**α), *N*-propionylbenzamide (**3**), and *N*-butyrylbenzamide (**4**), were also found to crystallize in the ct conformation. These imides are unsymmetrical and have two possible ct conformations, only one of which is found in their crystal structures.[22] The same ct conformation, with the acyl carbonyl group syn and the benzoyl carbonyl group anti with respect to the NH, is also present in their complexes. Another polymorph of *N*-acetylbenzamide (**2**β) and imides **5**–**11** crystallize in the tt conformation. The tt conformation of dibenzamide (**5**) is retained in its complexes.

Crystallographic Studies of Acyclic Imide Cocrystals. X-ray crystal structure analyses of cocrystals of the previous imides were performed when suitable single crystals could be obtained and definitive characterization of the hydrogen bond patterns was needed. Comparative hydrogen bond geometries and selected intra- and intermolecular bond lengths are given in Table III.

The ct conformations of **1** and **4** are retained in their cocrystal structures, **12**–**15**. These cocrystals, shown in Figures 1 and 2, consist of planar imide molecules that form centrosymmetric dimers, like those found in plain diacetamide (α form), linked by NH···O hydrogen bonds to the cis imide carbonyl groups. Except for the trans carbonyl and adjacent C–N bond lengths, the bond lengths and angles of diacetamide and *N*-butyrylbenzamide are very similar in their homomeric structures and in their cocrystals, **12**, **13**, and **15**. The anti lone pairs of electrons of the trans imide carbonyls are hydrogen bonded in the cocrystals **12**, **13**, and **15** to the –OH groups of *p*-nitrophenol or hydroquinone. The –OH groups of hydroquinone hydrogen bond to the syn lone pair of electrons in **14**, however. An unexpected increase of 0.008 Å for the cis carbonyl bond length and decrease of 0.009 Å for the adjacent C–N bond length occurs in this cocrystal. The phenol molecules are coplanar with the imide dimers in each of these cocrystals.

Planar ct molecules of **1** form imide–acid and imide–amide heterodimers in **16** and **17** in contrast to the imide···imide dimers in **1**, **3**, **4**, and **12**–**15**. The heterodimers, which are shown in Figure 3a,b, are linked into chains by OH···O hydrogen bonds between the trans carbonyl group and the phenolic hydroxyl group of the guest. An additional hydrogen bond between the anti lone pair of electrons of the cis imide carbonyl group and the trans NH of the amide relates two hydrogen-bonded chains by a pseudoinversion center in **17**.

The ct conformation of *N*-acetylbenzamide (**2**), *N*-propionylbenzamide (**3**), and the tt conformation of dibenzamide (**5**) are retained in their respective triphenylphosphine oxide (TPPO) cocrystal structures, **18**–**20** (Figure 4a–c). The imide fragments are not quite planar in **18**–**20** as indicated by the C–N–C–O torsion angles of 166.0 and 6.8°, 170.5 and 6.6°, and 21.3 and 13.4°, respectively. The phosphoryl oxygen, rather than the imide carbonyl groups, is the sole hydrogen bond acceptor in these cocrystals. The P=O bond length increases up to 0.010 Å as a consequence of complexation with **5** but does not change significantly upon complexation with **2** or **3**.[23] The imides adapt to the bulky guest molecule by twisting their phenyl groups from the plane of the imide π systems by 29.4° in **18**, 22.1° in **19**, and 15.4 and 28.5° in **20**. This conformational adaptation is similar to those observed in diarylureas when they complex with TPPO.[2]

The imide carbonyl bond lengths increase by 0.004–0.017 Å when hydrogen bonded to guest donors, as in **12**–**17**. The cor-

(16) The notation used in graph set analysis is $G_d^a(r)$. The pattern designator, G, is assigned as S, intramolecular (or self), D, a noncyclic finite pattern (e.g., a dimer), R, a cyclic finite pattern (ring), or C, an infinite pattern (chain). The parameters *a* and *d* refer to the number of acceptors and donors participating in the hydrogen bond, respectively. The degree or "size" of the pattern (*r*) is given in parentheses. For a detailed discussion of graph set analysis, see: Etter, M. C.; MacDonald, J. C.; Bernstein, J. *Acta Crystallogr.* **1990**, *B46*, 256–262.

(17) (a) Noe, E.; Raban, M. *J. Am. Chem. Soc.* **1975**, *97*, 5811–5820. (b) Hvoslef, J.; Tracy, M. L.; Nash, C. P. *Acta Crystallogr.* **1986**, *C42*, 353–360.

(18) Radom, L.; Riggs, N. V. *Aust. J. Chem.* **1980**, *33*, 2337–2342.

(19) Matias, P. M.; Jeffrey, G. A.; Ruble, J. R. *Acta Crystallogr.* **1988**, *B44*, 516–522.

(20) Kuroda, Y.; Taira, Z.; Uno, T.; Osaki, K. *Cryst. Struct. Commun.* **1975**, *4*, 321–324.

(21) Gentile, P. S.; Shankoff, T. A. *J. Inorg. Nucl. Chem.* **1965**, *27*, 2301–2309.

(22) Etter, M. C.; Britton, D.; Reutzel, S. M. *Acta Crystallogr.* **1990**, *C46*, in press.

(23) (a) Brock, C. P.; Schweizer, W. B.; Dunitz, J. D. *J. Am. Chem. Soc.* **1985**, *107*, 6964–6970. (b) Spek, A. L. *Acta Crystallogr.* **1987**, *C43*, 1233–1235.

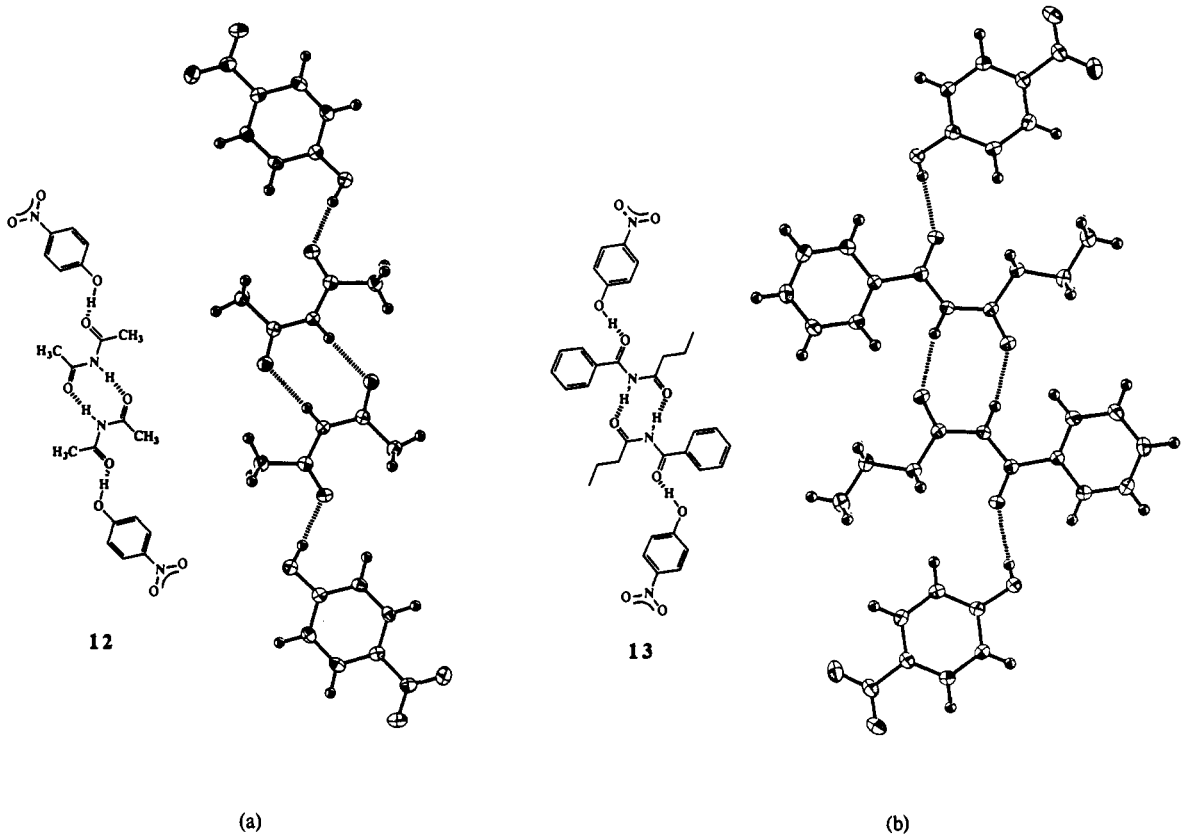

Figure 1. Tetrameric cocrystal hydrogen bond pattern formed by appending nitrophenols to the trans carbonyl groups of (a) diacetamide dimers, and (b) *N*-butyrylbenzamide dimers.

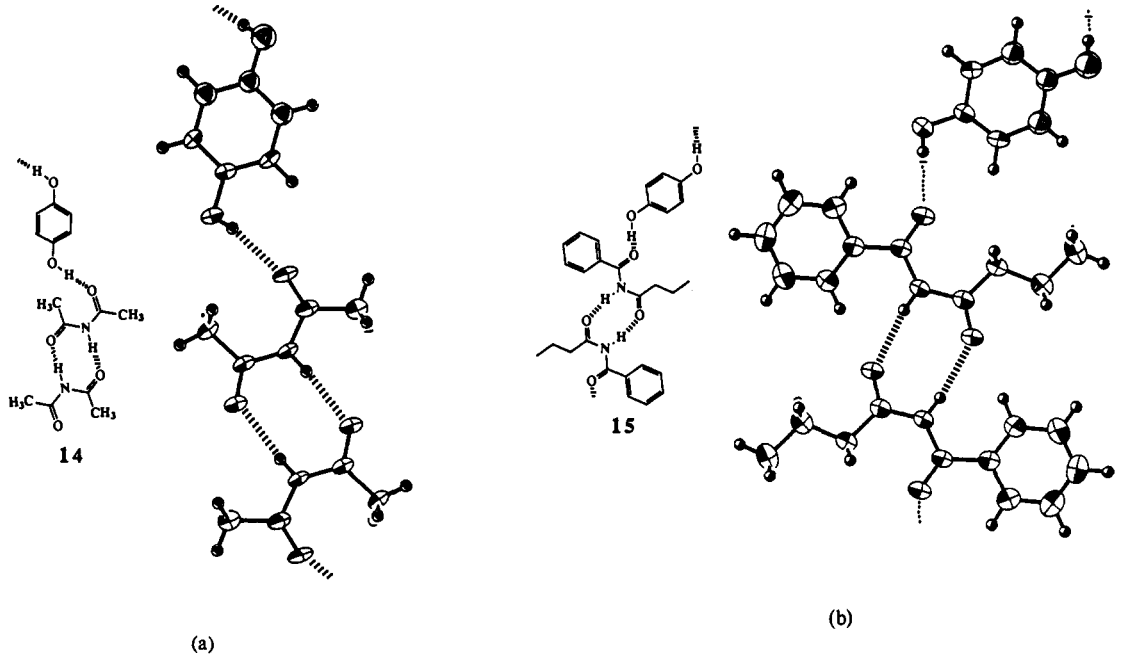

Figure 2. Infinite polymeric cocrystal hydrogen bond chains formed by appending bifunctional hydroquinone molecules to (a) diacetamide dimers, and (b) *N*-butyrylbenzamide dimers.

responding C–N bond lengths decrease by 0.004–0.021 Å. These structural changes are analogous to those caused by hydrogen bonding in amides.[24] The most important structural effect of the complexation of **2**, **3**, or **5** with TPPO is to cause the carbonyl groups to lose the hydrogen bonds that are present in their homomeric structures. As a result, these carbonyl bond lengths should decrease and the adjacent C–N bond lengths should increase relative to their values in their homomeric crystal forms. For **18** and **20**, the carbonyl bond lengths do decrease (by 0.007 Å in **18** and by 0.056 and 0.064 Å in **20**) and the C–N bond lengths do increase (by 0.009 Å in **18** and by 0.005 and 0.012 Å in **20**) upon complexation with TPPO. In **19**, however, no significant bond length differences were observed for imide molecules in their homomeric or cocrystal structures.

(24) (a) Jeffrey, G. A.; Ruble, J. R.; McMullan, R. K.; DeFrees, D. J.; Binkley, J. S.; Pople, J. A. *Acta Crystallogr.* **1980**, *B36*, 2292–2299. (b) Jeffrey, G. A.; Ruble, J. R.; McMullan, R. K.; DeFrees, D. J.; Pople, J. A. *Acta Crystallogr.* **1981**, *B37*, 1885–1890. (c) Stevens, E. D. *Acta Crystallogr.* **1978**, *B34*, 544–551.

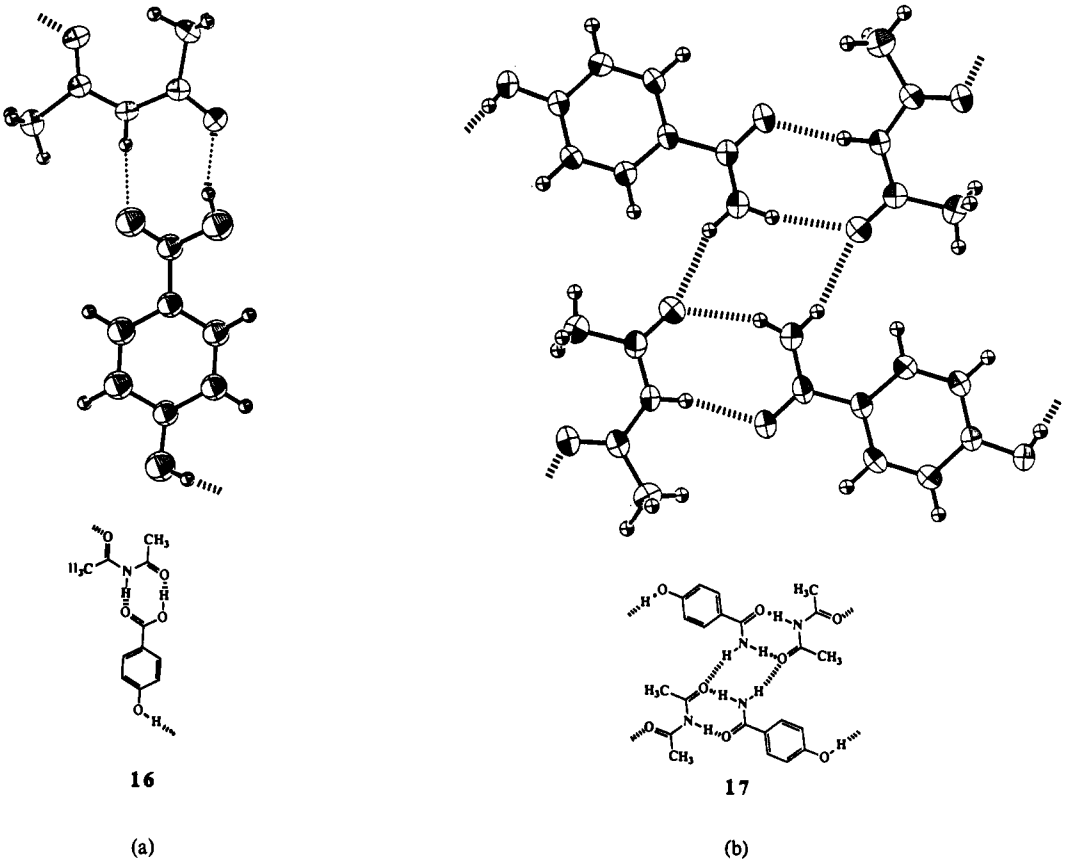

16 17

(a) (b)

Figure 3. Diacetamide heterodimers formed by replacing a diacetamide molecule in a homodimer with a better hydrogen bond donor such as (a) benzoic acid or acceptor such as (b) benzamide.

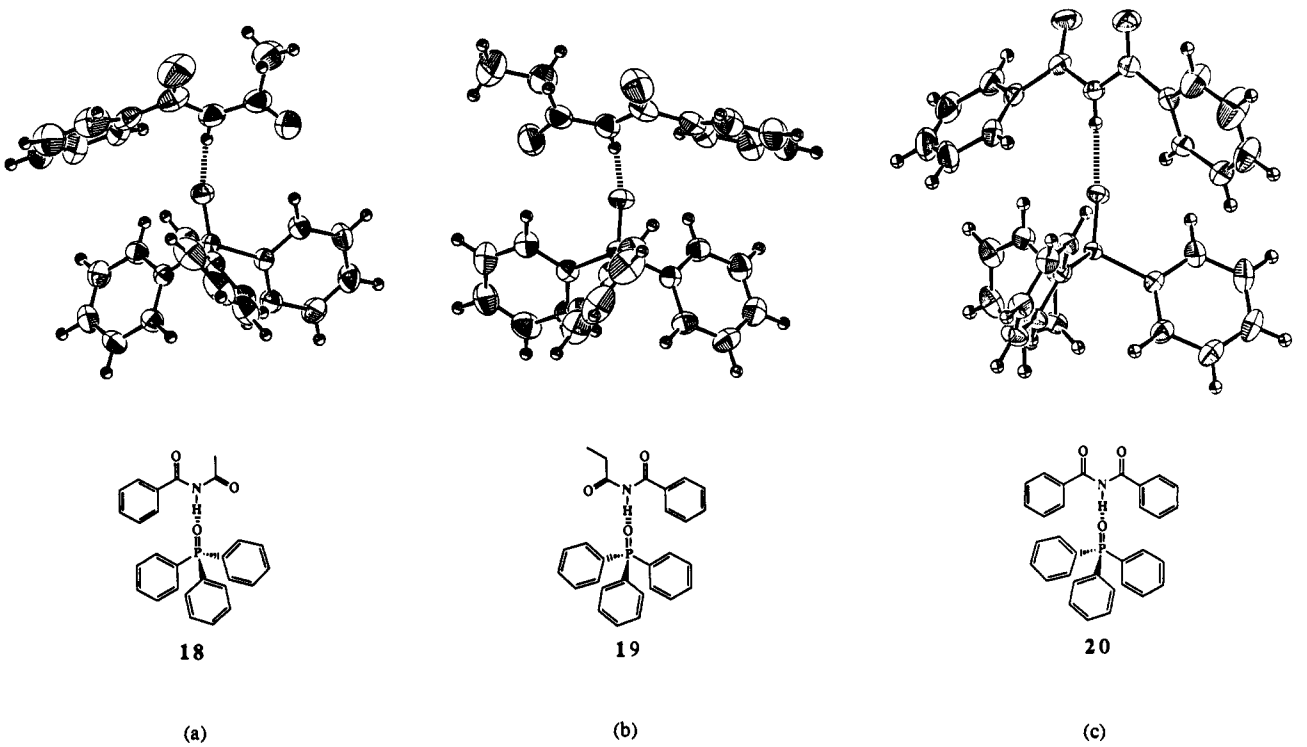

18 19 20

(a) (b) (c)

Figure 4. Phosphine oxide replaces the acyl carbonyl oxygens of (a) *N*-acetylbenzamide and (b) *N*-propionylbenzamide and both carbonyl oxygens of (c) dibenzamide as the hydrogen bond acceptor to the imide NH.

Noncrystallographic Methods for Characterizing Cocrystals. The experimental challenge in characterizing cocrystals is to determine whether the solid-state material obtained from a crystallization experiment is homogeneous or not, whether it contains any cocrystalline materials, and what the composition of the cocrystalline phase is. When nice single crystals make up the solid phase, then microscopy is a good indicator of overall homogeneity. A single crystal can often be extracted for further analysis of composition. New crystal forms may be observed even if they are not cocrystals. For example, polymorphs or solvates

Table II. Crystallographic Data for **12–20**

compd	**12**	**13**	**14**	**15**	**16**	**17**	**18**	**19**	**20**
formula	$C_{10}H_{12}N_2O_5$	$C_{17}H_{18}N_2O_5$	$C_{14}H_{20}N_2O_6$	$C_{28}H_{32}N_2O_6$	$C_{11}H_{14}N_2O_4$	$C_{11}H_{13}NO_5$	$C_{27}H_{24}NO_3P$	$C_{28}H_{26}NO_3P$	$C_{32}H_{26}NO_3P$
fw	240.22	330.34	312.32	492.57	238.24	239.23	441.47	455.49	503.54
space group	$P\bar{1}$	$P\bar{1}$	$P\bar{1}$	$P\bar{1}$	$P2_1/n$	$P\bar{1}$	$P\bar{1}$	$P\bar{1}$	$P2_1/c$
a (Å)	7.296 (4)	7.895 (8)	5.095 (6)	5.454 (3)	12.853 (7)	5.202 (2)	9.981 (5)	10.027 (3)	14.864 (4)
b (Å)	8.097 (2)	8.319 (3)	8.062 (5)	11.064 (7)	13.490 (3)	8.569 (4)	11.040 (7)	11.008 (4)	9.012 (1)
c (Å)	11.001 (7)	12.614 (7)	9.977 (4)	12.219 (3)	13.884 (2)	13.561 (2)	11.865 (3)	12.505 (4)	20.904 (7)
α (deg)	110.930 (4)	77.19 (4)	83.50 (4)	113.80 (2)		74.83 (2)	102.55 (4)	104.51 (3)	
β (deg)	107.460 (4)	89.10 (6)	88.82 (6)	96.38 (3)	101.49 (4)	87.39 (2)	101.80 (3)	99.91 (3)	109.97 (2)
γ (deg)	95.850 (3)	88.32 (5)	71.29 (7)	101.24 (5)		86.12 (3)	108.38 (5)	109.33 (3)	
V (Å^3)	562.9 (8)	807 (2)	386 (1)	647 (1)	2359 (2)	581.9 (7)	1156 (2)	1211 (2)	2632 (2)
Z	2	2	1	1	8	2	2	2	4
d_{calc} (g/cm^3)	1.417	1.359	1.345	1.265	1.341	1.365	1.268	1.249	1.271
crystl size (mm)	0.45 × 0.50 × 0.60	0.45 × 0.35 × 0.25	0.60 × 0.45 × 0.30	0.60 × 0.50 × 0.50	0.60 × 0.30 × 0.50	0.60 × 0.50 × 0.50	0.60 × 0.30 × 0.25	0.55 × 0.50 × 0.35	0.60 × 0.50 × 0.30
μ(Mo Kα) (cm^{-1})	1.08	0.95	0.99	0.83	0.97	1.02	1.41	1.37	1.33
T (°C)	−85 (1)	−64 (1)	24 (1)	24 (1)	23 (1)	24 (1)	23 (1)	22 (1)	−60 (1)
no. unique data total	2713	3877	1517	2275	5334	2800	4509	4246	5368
no. data used	2074	2436	1153	1598	2587	1715	3407	2691	3493
R^a	0.049	0.060	0.061	0.050	0.056	0.067	0.047	0.042	0.052
R_w^b	0.065	0.077	0.079	0.068	0.065	0.099	0.056	0.052	0.070
$2\theta_{max}$ (deg)	55.9	56	51.9	49.9	53.9	55.9	52.1	49.9	51.9
range of hkl	$-7 \le h \le 9$ $-10 \le k \le 10$ $-14 \le l \le 13$	$0 \le h \le 10$ $-10 \le k \le 10$ $-16 \le l \le 16$	$0 \le h \le 4$ $-8 \le k \le 9$ $-12 \le l \le 12$	$-6 \le h \le 3$ $-13 \le k \le 12$ $-13 \le l \le 14$	$0 \le h \le 16$ $0 \le k \le 16$ $-17 \le l \le 17$	$-5 \le h \le 6$ $-11 \le k \le 11$ $-17 \le l \le 17$	$0 \le h \le 12$ $-13 \le k \le 12$ $-14 \le l \le 13$	$0 \le h \le 11$ $-13 \le k \le 12$ $-14 \le l \le 14$	$0 \le h \le 18$ $-11 \le k \le 10$ $-25 \le l \le 24$
$(\text{shift/error})_{max}$	0.02	0.04	0.01	0.01	0.07	0.10	0.05	0.04	0.01
largest peak (e$^-$/Å^3)	0.26	0.37	0.31	0.20	0.26	0.28	0.44	0.28	0.27
graph set	$N_1 = R_2^2(8)D$	$N_1 = R_2^2(8)D$	$N_1 = R_2^2(8)D$ $N_2 = C_4^4(17)$	$N_1 = R_2^2(8)D$ $N_2 = C_4^4(17)$	$N_1 = DDD$ $N_2 = R_2^2(8)$	$N_1 = DDD$ $N_2 = R_2^2(8)$ $N_3 = R_4^2(8)$	$N_1 = D$	$N_1 = D$	$N_1 = D$

$^a R = \sum||F_o| - |F_c||/\sum|F_o|$. $^b R_w = [(\sum w(|F_o| - |F_c|)^2/\sum wF_o^2)]^{1/2}$; $w = 4F_o^2/\sigma^2(F_o^2)$.

Table III. Hydrogen Bond Geometries and Selected Intra- and Intermolecular Bond Lengths for **12–20**

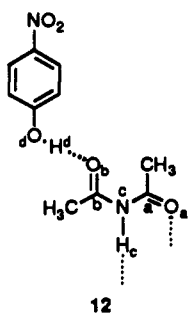
12

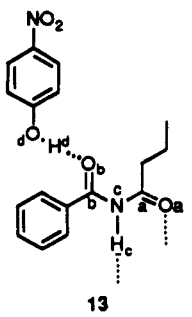
13

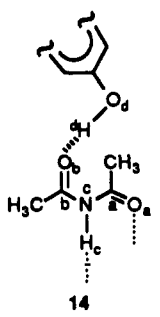
14

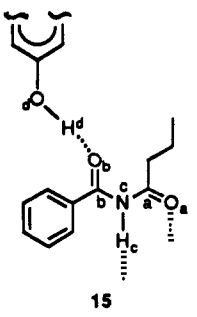
15

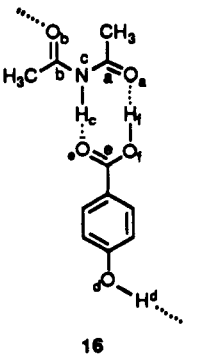
16

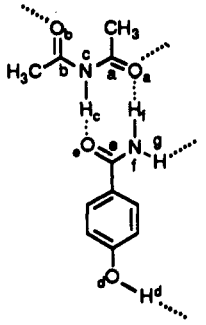
17

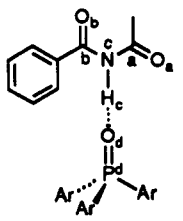
18

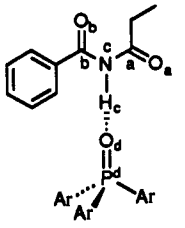
19

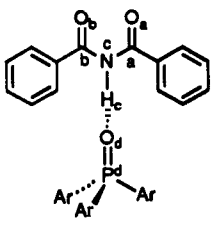
20

	12	13	14	15	16	17		18	19	20
$C_a{=}O_a$ (Å)	1.223 (2)	1.218 (3)	1.231 (3)	1.216 (3)	1.217 (3)	1.217 (4)	1.221 (4)	1.207 (3)	1.216 (3)	1.205 (4)
$C_b{=}O_b$ (Å)	1.225 (2)	1.228 (3)	1.215 (3)	1.217 (3)	1.221 (3)	1.217 (4)	1.219 (4)	1.214 (3)	1.222 (3)	1.209 (4)
$C_e{=}O_e$ (Å)					1.209 (3)	1.238 (4)	1.237 (3)			
$P_d{=}O_d$ (Å)								1.480 (2)	1.483 (2)	1.493 (2)
$C_a{-}N_c{-}C_b$ (deg)	130.1 (1)	129.6 (2)	130.7 (2)	129.7 (2)	129.6 (2)	129.3 (3)	129.2 (3)	128.7 (3)	128.7 (3)	123.9 (3)
$N_c{-}C_a{-}O_a$ (deg)	117.7 (1)	116.9 (2)	117.6 (2)	117.1 (2)	118.2 (2)	117.9 (3)	118.1 (3)	122.0 (3)	118.6 (3)	121.9 (3)
$N_c{-}C_b{-}O_b$ (deg)	122.8 (2)	120.9 (2)	123.6 (2)	120.8 (2)	122.4 (2)	122.4 (3)	122.4 (3)	118.8 (2)	122.7 (3)	123.2 (3)
$N_c{\cdots}O_{a,d,ore}$ (Å)	2.912 (2)	2.973 (3)	2.952 (4)	3.012 (3)	2.842 (3)	2.871 (4)	2.878 (4)	2.839 (3)	2.836 (3)	2.897 (3)
$H_c{\cdots}O_{a,d,ore}$ (Å)	2.08 (2)	2.08 (3)	2.12 (4)	2.17 (3)	2.00 (4)	2.014	2.034	2.02 (3)	1.96 (3)	2.03 (4)
$N_c{-}H_c{\cdots}O$ (deg)	174.0 (1)	161.5 (1)	176 (3)	167.5 (1)	175.3 (1)	173.0 (1)	166.4 (1)	171 (3)	172 (3)	164.4 (1)
$O_d{\cdots}O_b$ (Å)	2.690 (2)	2.685 (3)	2.832 (4)	2.777 (3)	2.703 (3)	2.730 (4)	2.728 (4)			
$H_d{\cdots}O_b$ Å	1.85 (3)	2.04 (4)	2.14 (4)	2.02 (3)	1.97 (6)	2.04 (1)	1.99 (1)			
$O_d{-}H_d{\cdots}O_b$ (deg)	173.9 (1)	176.0 (1)	165 (3)	170.6 (1)	140.5 (1)	171.1 (1)	172.2 (1)			
$O_a{\cdots}O_f$ (Å)					2.715 (3)					
$O_a{\cdots}N_f$ (Å)						3.007 (4)	2.974 (5)			
$H_f{\cdots}O_a$ (Å)					1.93 (6)	2.133	2.179			
$O_f{-}H_f{\cdots}O_a$ (deg)					149.2 (1)					
$N_f{-}H_f{\cdots}O_a$ (deg)						166.0 (1)	145.8 (1)			
$N_f{-}H_g{\cdots}O_a$ (deg)						159.6 (1)	157.5 (1)			

of the reagents might form or even just a new crystal morphology of one of the starting materials could form. The problem when working with single crystals is to know whether they are representative of the bulk material. If large single crystals are not evident, then the problem is more difficult. All analyses necessarily involve many particles, some of which might be cocrystals. It is not the purpose of this paper to describe the general analytical strategies for studying organic solids, rather to show a few examples of how noncrystallographic analytical methods were used to solve the problem of characterizing imide cocrystals.

Cocrystals **21–31** have been prepared and characterized by chemical and spectroscopic means other than by crystallography. Except for **28** and **31**, we were able to determine their hydrogen bond patterns unambiguously. The proposed hydrogen bond aggregates of most of the cocrystals for which X-ray crystal structure analyses have not been done are based on spectroscopic evidence and are shown in Figure 5.

Characterization of the chemical composition of the cocrystals and their hydrogen bond patterns was based on melting point analysis, solid-state IR, solution-state ^1H and ^{13}C NMR, ^{13}C and ^{31}P CP/MAS NMR, and X-ray powder diffraction. Solid-state NMR was particularly useful in characterizing the imide cocrystals.[25] Since carbonyl carbon chemical shifts are sensitive to hydrogen bonding, complexation could be monitored by comparing the carbonyl ^{13}C shifts of the cocrystal relative to those of the host imide in the solid state.[26] Solid-state IR proved to be a particularly reliable tool for discriminating between possible imide conformers.[27] The other techniques were used for supporting evidence of cocrystal formation.

The crystal structures of **12–15** showed that the cis imide carbonyl groups were hydrogen bonded in both their homomeric as well as their cocrystal forms, but that the trans imide carbonyl groups were hydrogen bonded only in their cocrystal phases. Thus, one would expect complexation to cause large downfield NMR shifts for the trans carbonyl carbons but small or no shifts for the cis carbonyl carbons. When **1**, **3**, and **4** are complexed with para-substituted phenols, usually only one of their two NMR carbonyl carbon resonances shifted downfield (by 2–5 ppm), so those peaks were assigned to the trans imide carbonyl carbons.

(25) Details of the ^{13}C CP/MAS NMR characterization of the imide cocrystals will be reported in a future report.
(26) Etter, M. C.; Hoye, R. C.; Vojta, G. M. *Cryst. Rev.* **1988**, *1*, 281–338.
(27) Uno, T.; Machida, K. *Bull. Chem. Soc. Jpn.* **1961**, *34*, 551–556.

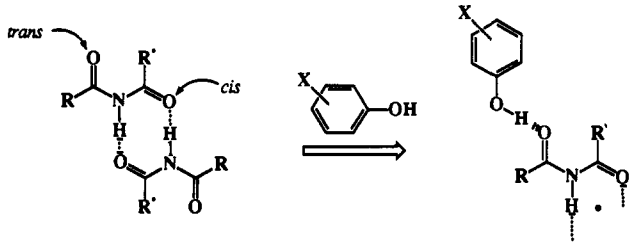

The remaining carbonyl peaks that did not move were attributed to the cis carbonyl carbons. In **14**, no significant change in either of the carbonyl carbon chemical shifts occurred. Solid-state NMR was not sensitive enough to detect the weak OH···O hydrogen bond. The O···O hydrogen bond length in **14** (2.832 (4) Å) is longer than that usually observed in the imide–phenol complexes (2.685–2.730 Å). Other ct amide cocrystals with phenols substituted with Br, Cl, NO_2, or OH (**21–26**) showed the usual spectral shifts relative to their host imides, so it is proposed that these structures have the patterns shown in Figure 5.

Interpretation of the solid-state NMR spectra of cocrystals of **1** with carboxylic acids and amides was sometimes complicated by overlapping carbonyl peaks of the hosts and guests. In most cases, a downfield shift (2–3 ppm) of one of the imide carbonyls was observed, although characterization of the precise hydrogen bond patterns was not possible from this data alone.

Solid-state NMR provided critical information for characterizing the 1:1 cocrystal between **1** and 3,4-dinitrobenzoic acid (**30**) (Figure 6).[25] Upon complexation with 3,4-dinitrobenzoic acid, the trans carbonyl carbon peak of **1** shifted 3 ppm downfield, while the cis carbonyl carbon peak did not move. Both imide carbonyl groups therefore must be hydrogen bonded in the cocrystal. Simultaneously, the carboxyl carbon peak of 3,4-dinitrobenzoic acid shifted 7 ppm upfield compared to its position in its own crystal structure (where it is a hydrogen bonded dimer),[28] clearly indicating that the carbonyl group is no longer hydrogen bonded in the cocrystal. The proposed hydrogen bond aggregate that accounts for these chemical shift changes is shown in Figure 5. This pattern is analogous to those of **12**, **13**, and **21–25**.

Evidence for the structure of the hydyrogen bonded aggregate in the dibenzamide–TPPO complex (**20**) was also provided by ^{13}C CP/MAS NMR. The carbonyl carbon chemical shifts in the cocrystal were 2 and 5 ppm upfield, respectively, compared to their homomeric structures, indicating that they were probably no longer hydrogen bonded. The presence of two peaks also indicated that the carbonyls are no longer crystallographically equivalent. This interpretation was subsequently confirmed by the X-ray crystal structure of **20**.

By comparing the relative intensities of the coupled symmetric and asymmetric amide C=O bands of the imides, which are usually in the ratio of ~50:1, IR spectroscopy was used to determine which imide conformer was present in the cocrystals.[27] The relative band intensities in **2α** and **3** remained unchanged upon complexing TPPO, indicating that the ct imide conformation was retained in **18** and **19**, respectively (Figure 4). This hypothesis was later confirmed by X-ray crystallography. The ct conformation of **2** and **3** is observed despite possible electrostatic repulsion between the acetyl oxygen and the near-neighbor phosphoryl oxygen.

Hydrogen Bond Patterns of Acyclic Imides and Their Cocrystals. The simple ct imides **1–4** form cyclic hydrogen bonded dimers. In this aggregate, one of the carbonyl groups is not used in hydrogen bonding. This dimer behaves like a bifunctional acceptor, shown schematically, in its cocrystallization properties.

We proposed that the non-hydrogen-bonded carbonyl groups of these dimers would be available to serve as sites for hydrogen bonding to proton donor guests, such as phenols. Indeed, not only

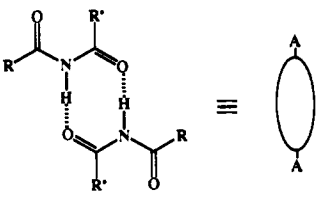

was it possible to form such cocrystals, but their aggregate patterns could be controlled by choosing guest molecules with appropriate numbers and orientations of proton donor groups. Heteromeric tetramers or infinite chains were prepared according to the scheme shown below where A is the imide carbonyl acceptor and –DH is a guest proton donor.

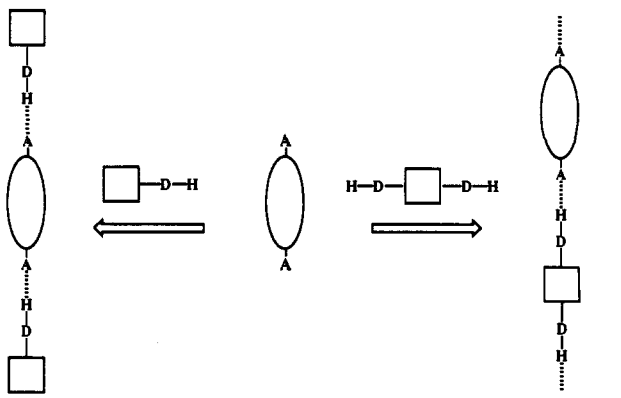

Finite hydrogen-bonded aggregates were prepared by cocrystallizing monophenols with the ct imide dimers of **1**, **3**, and **4**. Seven 1:1 cocrystals of this type, including **12** and **13** (Figure 1a,b), were prepared. The OH···O hydrogen bonds between the trans imide carbonyl groups and the phenolic OH's are the driving force for cocrystal formation. Infinite hydrogen-bonded chains were formed by linking imide dimers of **1**, **3**, and **4** with diphenols, analogous to the preparation of copolymers using two difunctional reagents. Three 2:1 cocrystals, including **14** and **15** (Figure 2a,b), have been prepared with this type of hydrogen bond pattern.

N-Acetylbenzamide (**2**) exists as cyclic hydrogen-bonded dimers in its α polymorph but does not behave like the other ct imides toward proton donor guests. Under the standard conditions (methods A and B) used for obtaining cocrystals, the tt polymorph, β, is obtained rather than cocrystals with phenols. These results indicate that the cocrystallization properties of **2** are dictated by the tt polymorph, β, rather than the ct polymorph, α.

The 1:1 cocrystals between imides **1**, **3**, and **4** and para-substituted phenols form with phenols that have NO_2, Br, Cl, or CN groups as substituents. These substituents are weak acceptors and do not compete with imide carbonyl groups for the available hydrogen bond donors in the cocrystals. When the para-substituents are carboxylic acids or amides, however, the hydrogen-bonded aggregates change dramatically as these functional groups provide competitive hydrogen-bonding sites. Cyclic eight-membered ring heterodimers form in preference to the imide dimers discussed previously when **1** is crystallized with a primary amide or an acid, as in **16** and **17** (Figure 3a,b). Imide···guest heterodimers are linked into chains by OH···O hydrogen bonds between carbonyl groups and phenolic hydrogens. When an amide replaces an acid group, as in **17**, an additional hydrogen bond donor is added to the system. It is accommodated in the same way as the extra hydrogen in homomeric primary amide structures by bonding as the second hydrogen bond donor to the anti lone pairs of electrons of a neighboring carbonyl group.[6] The tetramers resulting from these interactions in **17** are linked into infinite chains by the phenol –OH groups bonding to the unused diacetamide carbonyl groups (O(1)).

The complexing behavior of ct imides is distinctly different toward various classes of proton donors. Whereas **1** forms co-

(28) 3,4-Dinitrobenzoic acid crystallizes as hydrogen-bonded dimers as determined by solid-state IR spectroscopy. For determination of hydrogen-bonded chain vs dimers by solid-state IR, see: Walborsky, H. M.; Barash, L.; Young, A. E.; Impastato, F. J. *J. Am. Chem. Soc.* **1961**, *83*, 2517–2525.

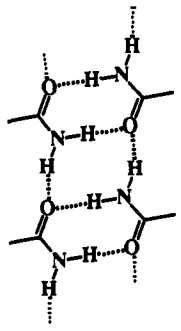

primary amide chains

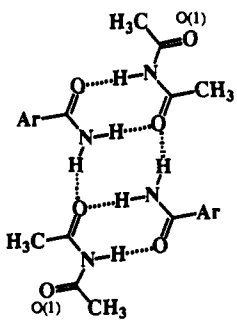

diacetamide - amide tetramers

crystals with many different classes of proton donors, **3** and **4** form cocrystals only with phenol donors. It is also difficult to cocrystallize the ct imides **1**, **2α**, **3**, and **4** with most acceptors. Two examples, however, are the 1:1 complexes of **2** and **3** with TPPO, **18** and **19**, respectively (Figure 4a,b). The NH groups of **2** and **3** preferentially form hydrogen bonds to the phosphoryl oxygen of TPPO rather than to their own carbonyl groups, thus preventing the formation of the cyclic dimers found in their homomeric structures **2α** and **3**, respectively. The other ct imides, **1** and **4**, do not complex with TPPO.

The complexing behavior of tt imides reflects both the conformational and hydrogen bonding preferences of these imides. Imides that adopt the tt conformation in their homomeric crystal forms almost always form infinite chains linked by bifurcated hydrogen bonds. The only acyclic imide that has the tt conformation and does not form bifurcated hydrogen-bonded chains is **2β**. It forms chains linked by NH···O hydrogen bonds to only the benzoyl carbonyl groups. The acetyl carbonyl oxygen atom is 3.069 Å from the nearest intermolecular NH hydrogen atom. The imide moiety (–CO–NH–CO–) is nonplanar as indicated by the O(1)–C(1)–N–C(2) and O(2)–C(2)–N–C(1) torsion angles of 11.1 (3) and 13.9 (3)°, respectively.

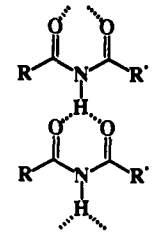

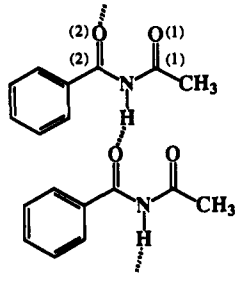

Imides adopting the tt conformation did not form cocrystals with hydrogen bond donor guests, such as phenols, carboxylic acids or amides, but a few of them did complex the best hydrogen bond acceptors. As previously mentioned, TPPO is a guest hydrogen bond acceptor for **2**, which is tt in the β form, in cocrystal **18** (Figure 4a). TPPO is also a guest acceptor to **5** in its cocrystal **20** (Figure 4c). These cocrystals of tt imides are rare since we found that neither tt diacylamines nor tt acylbenzamides with bulky acyl groups would complex TPPO.

Cocrystallization Process. Both solid-state and solution cocrystallizations of all the host–guest pairs were attempted. Cocrystals were not always obtained by both methods. Solid-state grinding afforded cocrystals of **28** and **30** when their solution-state cocrystallizations were unsuccessful. The inability to isolate cocrystals from solution when they could be readily obtained in the solid state is frequently due to different solubilities of the components, so the solid-state grinding method proved to be the best indicator of potential cocrystal formation.

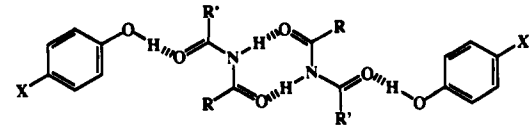

Cmpd	R	R'	X
21	Et	Ph	NO_2
22	Me	Me	CN
23	Pr	Ph	Br
24	Et	Ph	Br
25	Pr	Ph	Cl

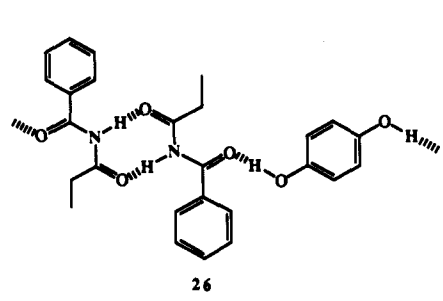

26

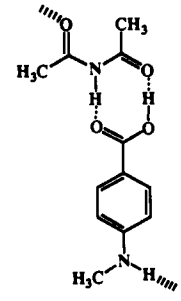

29

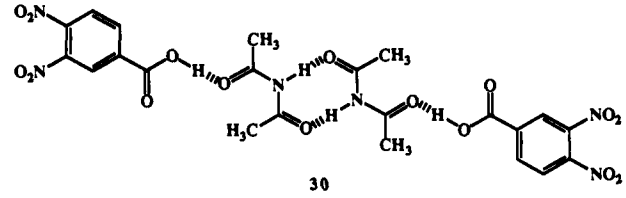

30

Figure 5. Proposed hydrogen-bonded aggregates for **21–26**, **29**, and **30** on the basis of chemical and spectroscopic data.

Typically, from one to three common solvents or solvent pairs were used in the recrystallization experiments. Some cocrystals that were expected to form on the basis of previous successful cocrystallizations of related host–guest pairs did not form by either solid-state grinding or solution recrystallizations. In such cases, evaporation rates, temperature, light vs darkness, and additional solvents were tested. These changes did not result in cocrystal formation, so for most of the host–guest pairs only the standard methods (methods A and B in Experimental Section) were used.

Discussion

The cocrystallization properties of acyclic imides depend on which conformation they adopt in their homomeric crystal forms. The cis–trans and trans–trans conformers found in imide crystal structures have their own unique hydrogen bond properties. The cis–trans forms behave like a combination of two independent functional groups: a primary amide (forming dimers) and a tertiary amide (acting as an acceptor only).

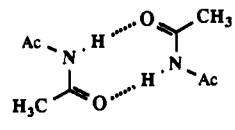

'Primary amide-like" portion

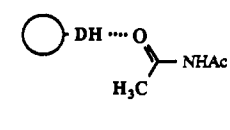

"Tertiary amide-like" portion

(O– DH is a guest donor)

Cis-trans Imides

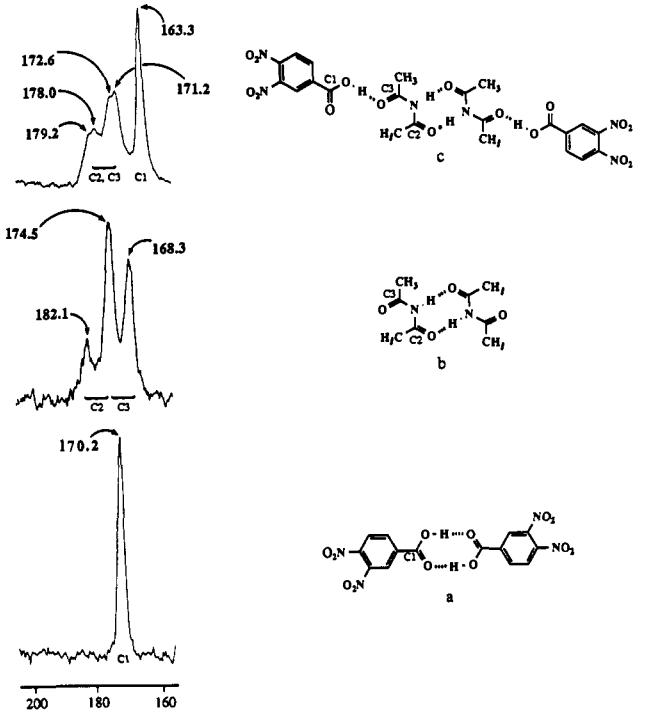

Figure 6. Carbonyl region of ^{13}C CP/MAS solid-state NMR spectra (25 MHz). The imide carbonyl peaks are split into asymmetric doublets due to the adjacent quadrupolar ^{14}N atoms. (a) 3,4-Dinitrobenzoic acid spectrum showing a single peak for the carbonyl carbon (C(1)) in a hydrogen bond pair. (b) Diacetamide spectrum (polymorph 1α) showing two partially overlapping doublets due to the carbonyl carbons in a hydrogen-bonded carbonyl group (C(2), 7 ppm downfield) and in a free carbonyl group (C(3)). (c) Diacetamide–acid cocrystal showing that both carbonyl carbons of diacetamide have nearly the same chemical shift (C(2), C(3) both 3–4 ppm downfield), so they are now both hydrogen-bonded, while the acid carbonyl peak (distinguishable as a singlet) has moved upfield since it is no longer hydrogen bonded in the cocrystal.

In trans–trans imides, the two carbonyl groups usually act like a bidentate ligand that complexes a proton donor. This pattern is like that of secondary amides with an additional acceptor ligand:

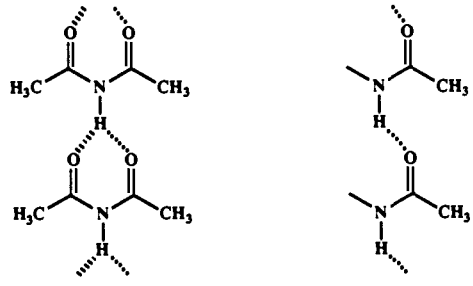

Trans-trans Imides *Secondary Amides*

The cocrystallization process can be viewed as a competition between homomeric aggregation and heteromeric aggregation. Consideration of how a hydrogen bond guest could compete with and displace the hydrogen bond pattern of the homomeric ct or tt forms prior to crystal nucleation is a useful way to predict imide cocrystallization patterns. If the imide aggregates with itself in a ct conformation, it will then have an unused carbonyl group as a site for complexation to proton donor guest molecules (cocrystals of this type are referred to as type I complexes). If the guest donor is itself capable of forming eight-membered ring hydrogen bonded chains, e.g., a primary amide or a carboxylic acid, then an alternative complexation mechanism would be to form the type II heterodimer cocrystal. The hydrogen bonded chains formed by tt imides that aggregate with themselves could be perturbed by guest molecules to give either type III or IV cocrystals (Figure 7).

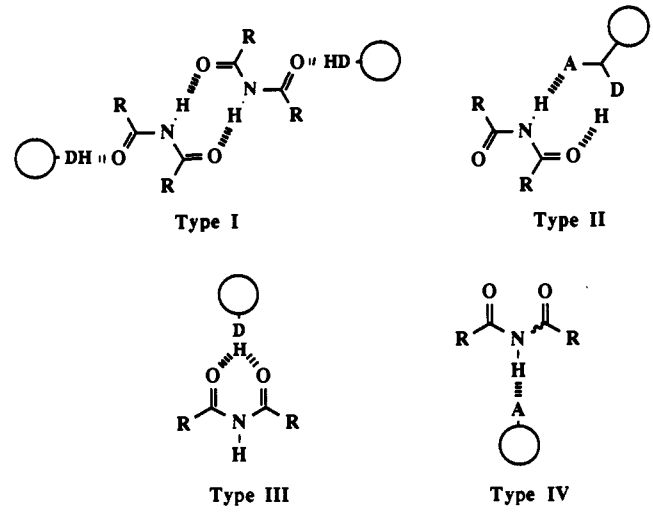

Figure 7. Acyclic imide cocrystal types. Types I and II are observed most frequently. Type III is surprisingly uncommon, indicating how difficult it is to disrupt hydrogen bond chains of tt imides. Type IV is observed only for TPPO complexes.

Type I Complexes (12–15, 21–26, 30). These cocrystals are observed most frequently for diacetamide or aryl–alkyl imides with phenols or carboxylic acids of high acidity. The imides that form type I cocrystals are found in the same ct conformation in their own homomeric crystal structures.

Type II Complexes (16,17,29). These cocrystals form when a strong carboxylic acid or a primary amide is used as a guest molecule. In these cases, the host and guest molecules are both capable of forming stable hydrogen bonded dimers. The driving force for cocrystallization in these cases may be that the heteromeric pairing involves a stronger hydrogen bond than those formed in the respective homomeric dimers.

Type III Complexes. The imide carbonyl groups have been used to chelate group I and II metal ions, but no organic donor molecules have been found to give a type III structure.

Type IV Complexes (18–20). These cocrystals were very difficult to form, occurring only in three cases where an exceptionally strong proton acceptor (TPPO) was used. Attempts were made unsuccessfully to cocrystallize TPPO with seven other imides. In light of our previous use of TPPO as a general cocrystallizing agent for proton donors,[1] these findings were unexpected. One implication is that the cost of breaking two imide NH···O=C bonds is too large to be compensated for by a strong NH···O=P bond.

Exceptions (27). The crystal structure of **27** has been reported previously.[19] In this structure, diacetamide and acetamide form hydrogen-bonded chains similar to those formed by secondary amides. The hydrogen-bonded chains are cross-linked by hydrogen bonds between the cis amide NH and the anti lone pair of electrons of the cis imide carbonyl group. This pattern has the expected features that diacetamide is in its ct conformation and all carbonyl groups and –NH hydrogens are used in the hydrogen bond patterns. What is unexpected is that neither diacetamide nor acetamide participate in any eight-membered ring hydrogen bond patterns in this structure.

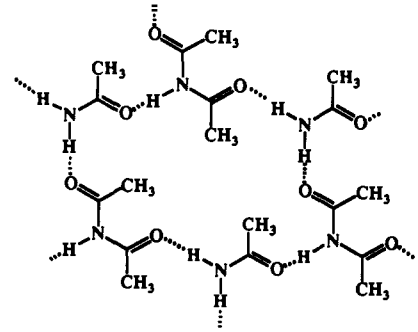

27

Table IV. Hydrogen Bond Rules for Acyclic Imides and Their Cocrystals

1 All alkyl and aryl acyclic imides that adopt the trans–trans conformation (8 in paper, 13 studied to date) form chains, usually involving bifurcated hydrogen bonds.
2 All alkyl and aryl acyclic imides that adopt the cis–trans conformation form eight-membered hydrogen-bonded ring dimers in their homomeric structures and in their cocrystals.
3 Hydrogen bond patterns form as if the best hydrogen bond donor paired with the best hydrogen bond acceptor first and subsequent hydrogen bonds were formed according to their relative donating and accepting abilities.
4 The imide donor and both acceptors are used in their cocrystals when possible.
5 Relative accepting abilities of imide groups and other functional groups present in imide crystals or cocrystals:

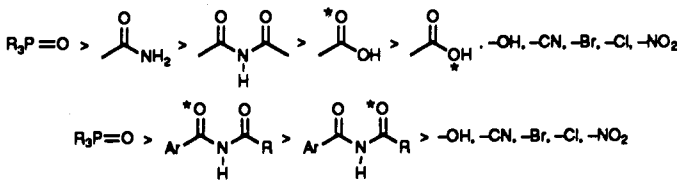

Hydrogen Bond Rules and Relative Proton-Donating and -Accepting Abilities. There are certain features common to hydrogen bond patterns in organic crystals in general and other features that are specific to different functional group classes.[8] We have found it useful, with a large number of crystal and cocrystal structures of one class of functional groups, to summarize their hydrogen bond patterns according to their topology and to their functional group selectivity. In the best cases, these summaries, or hydrogen bond rules, can be used as predictors of hydrogen bond patterns for new structures and as guidelines for designing new cocrystals and host–guest pairs.

The imide series presented here is the largest database we have yet analyzed. From just a handful of imide homomeric structures from the literature, an iterative process of predicting new structures based on that small database, preparing those compounds and their cocrystals, determining their structures, and then modifying the rules as dictated by the new data was followed. Certain hydrogen bond properties emerged repeatedly and became very useful for predicting new structures. These properties are listed in Table IV as hydrogen bond rules for acyclic imides and their cocrystals.

One of the most remarkable features of these rules is that the hydrogen bond connectivity patterns are based on functional group analysis only, as if *the crystal nucleation and growth processes do not perturb the preferred hydrogen bond connectivity patterns.* An example of this phenomenon is the ranking of relative accepting abilities of the various proton-accepting functional groups in the imide series (rule 5, Table IV). This ranking was derived from the empirically determined connectivity patterns in the crystal structures of **12–20** and in the proposed hydrogen bond patterns of **21–26**, **29**, and **30**. The rankings derive from assigning the best acceptor as either the only one that is used in the presence of other acceptors or the one that is bonded to the most acidic proton donor in a structure with several donors. For example, in **16** the calculated pK_a's are $-CO_2H$ (4.57), $-OH$ (9.23), and $-NH$ (11.8).[29] Thus, the best acceptor is assigned to the one bonded to the carboxylic acid hydrogen. Using this criterion, the best acceptor is the imide carbonyl group. This method has pitfalls since pK_a is not a direct measure of hydrogen bond abilities when comparing different kinds of functional groups and when working in nonaqueous media. Nevertheless, it is the best indicator of hydrogen bonding ability available, in lieu of α and β rankings determined by solvatochromatic measurements.[30] When pK_a differences are small and when there are multiple competing groups (i.e., more than two or three), then we expect these rankings will not be strictly observed in the solid state. Other cases where they may not be observed is when steric interference prevents the preferred contact from forming or when other intermolecular interactioins that are stronger than hydrogen bonds are present (e.g., ionic interactions). For example, 2,4-dinitrophenol does not complex with **1** in the usual type I pattern, presumably due to interference by the ortho nitro group.

Cocrystallization Phenomenon. The prior discussion has referred to observed hydrogen bond patterns in homomeric imides and their cocrystals, but many proposed cocrystal pairs could not be prepared at all. Diacetamide is an exception. It is a very versatile cocrystallizing agent, forming cocrystals from solution or in the solid state with many proton-donor and -acceptor guests.

Simply choosing a proton-donor host and an acceptor guest that can form a stronger hydrogen bond to one another than to themselves is not a sufficient condition for predicting when cocrystals will form. For example, 4-nitrobenzoic acid does not cocrystallize with diacetamide even though 3,4-dinitrobenzoic acid does (**30**). Other forces must be operating that prevent the cocrystallization of this host–guest pair. The inability of most imides to complex TPPO, thus forming strong NH···O=P hydrogen bonds, further demonstrates that optimizing donor and acceptor strengths does not necessarily result in cocrystal formation.

The cocrystallization process represents a balancing of all the forces impinging on a molecule in solution as well as in the solid state. Since most of the imide cocrystals that form do so either in the absence or presence of solvent, the solvent effects alone are not dictating which pairs of molecules will cocrystallize. Once cocrystals have formed, however, the heteromeric hydrogen bond rules presented previously can be used to predict their hydrogen bond patterns.

Use of Acyclic Imide Hydrogen Bond Rules in Biochemical Systems. We have shown how preferred imide hydrogen bond patterns are related to those of primary, secondary, and tertiary amides. It is also tempting to apply imide hydrogen bond rules to chemical homologues and analogues such as cyclic imides, uracils, and barbiturates and to investigate host–guest interactions of imide-type functional groups in DNA, protein, or enzyme receptor sites.[31] For small-molecule analogues, such as cyclic imides, the relationship between their hydrogen bond properties and those of acyclic imides is, however, not obvious. Despite the chemical homology of these classes of compounds, the fact that cyclic imides can adopt only the cc conformer but that acyclic imides prefer the tt conformer (occasionally ct is found, but never cc), is more important to their molecular recognition properties than are their chemical similarities. For example, succinimide forms typical hydrogen bonded dimers in its homomeric crystals,[32] but forms an unusual 1:1 cocrystal with hydroquinone.[33] By comparison, **14** and **15** (Figure 2a,b) form 2:1 cocrystals with

(29) Perrin, D. D.; Dempsey, B.; Serjeant, E. P. *pK_a Prediction for Organic Acids and Bases*; Chapman and Hall: London and New York, 1981.
(30) (a) Taft, R. W.; Kamlet, M. J. *J. Am. Chem. Soc.* **1976**, *98*, 2886–2894. (b) Kamlet, M. J.; Taft, R. W. *J. Am. Chem. Soc.* **1976**, *98*, 377–383. (c) Kamlet, M. J.; Abboud, J.-L. M.; Abraham, M. H.; Taft, R. W. *J. Org. Chem.* **1983**, *48*, 2877–2887.
(31) (a) Seeman, N. C.; Rosenberg, J. M.; Rich, A. *Proc. Nat. Acad. Sci. U.S.A.* **1976**, *73*, 804–808. (b) Pabo, C. O.; Sauer, R. T. *Annu. Rev. Biochem.* **1984**, *53*, 293–321. (c) Feibush, B.; Figueroa, A.; Charles, R.; Onan, K. D.; Feibush, P.; Karger, B. L. *J. Am. Chem. Soc.* **1986**, *108*, 3310–3318. (d) Buchet, R.; Sandorfy, C. *J. Phys. Chem.* **1984**, *88*, 3274–3282. (e) Kyogoku, Y.; Lord, R. C.; Rich, A. *Nature* **1968**, *218*, 69–72. (f) Voet, D.; Rich, A. *J. Am. Chem. Soc.* **1972**, *94*, 5888–5891. (g) Yu, N.-T.; Kyogoku, Y. *Biochim. Biophys. Acta* **1973**, *331*, 21–26.
(32) Mason, R. *Acta Crystallogr.* **1956**, *9*, 405–410.
(33) Unpublished results.

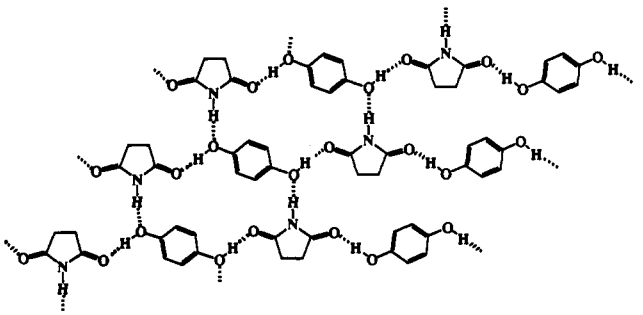

1:1 Cocrystal of a Cyclic Imide and Hydroquinone

hydroquinone. Thus, the hydrogen bond patterns of the cyclic or acyclic imide–hydroquinone complexes are completely different. We are currently studying the relationships between cyclic and acyclic imide cocrystal patterns and plan in the future to relate these systems to uracils.

Conclusions

The use of hydrogen bond interactions to direct selective molecular recognition processes of acyclic imides has been demonstrated by studying their cocrystallization properties. Acyclic imides retain their native conformation (as found in homomeric crystals) when interacting with guest molecules during the cocrystallization process. Host–guest pairs self-assemble in the absence of preorganized cavities according to relative hydrogen bond donating and accepting abilities of the functional groups that are present as well as according to the number and orientation of such groups. These results show that cocrystallization experiments provide a useful way to map out the molecular recognition properties of a class of molecules and to test for hydrogen bond selectivity in weakly associated, multifunctional systems.

Acknowledgment. We gratefully acknowledge Prof. Doyle Britton, Department of Chemistry, University of Minnesota, for his crystallographic assistance and the NIH (GM 42148-01) for financial support.

Supplementary Material Available: Positional parameters, anisotropic thermal parameters, intra- and intermolecular bond lengths and angles, and unit cell drawings for seven crystal structures (149 pages); tables of observed and calculated structure factors (147 pages). Ordering information is given on any current masthead page.

Use of Aza-Cope Rearrangement–Mannich Cyclization Reactions To Achieve a General Entry to *Melodinus* and *Aspidosperma* Alkaloids. Stereocontrolled Total Syntheses of (±)-Deoxoapodine, (±)-Meloscine, and (±)-Epimeloscine and a Formal Synthesis of (±)-1-Acetylaspidoalbidine

Larry E. Overman,* Graeme M. Robertson, and Albert J. Robichaud

Contribution from the Department of Chemistry, University of California, Irvine, California 92717. *Received June 29, 1990*

Abstract: The first total syntheses of the structurally unusual pentacyclic *Melodinus* alkaloids (±)-meloscine (**1**) and (±)-epimeloscine (**2**) and the hexacyclic *Aspidosperma* alkaloid (±)-deoxoapodine (**4**) are reported. The syntheses proceed via a highly functionalized common tetracyclic intermediate **7**, which is accessed (with complete stereocontrol) by the title rearrangement of pyrindinol **10**. These syntheses provide excellent examples of the power of tandem aza-Cope rearrangement–Mannich cyclization reactions as the key element of stereocontrolled alkaloid synthesis design.

In recent years we have developed a fundamentally new approach to alkaloid synthesis in which the facile [3,3]-sigmatropic rearrangement of iminium cations is combined with an intramolecular Mannich cyclization.[1] In the simplest case, a homoallylic amine with alkoxyl or hydroxyl substitution at the allylic site is allowed to react with an aldehyde or ketone in the presence of an equivalent or less of acid to yield a substituted 3-acylpyrrolidine product (eq 1).[2] If the starting amino alcohol is cyclic, the aza-Cope rearrangement–Mannich cyclization reaction affords a pyrrolidine annulated product in which the initial ring is expanded by one carbon. This latter transformation has been employed to provide a variety of cis fused hydroindoles, cyclopenta[*b*]pyrrolidines, and cyclohepta[*b*]pyrrolidines (eq 2)[3] as well as complex alkaloids of the *Dendrobatid*,[4] *Amaryllidaceae*,[5] and *Aspidosperma*[6] families.

Chart I

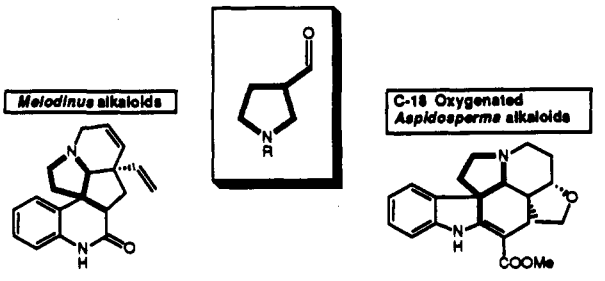

(1) Part 21 in the series *Synthesis Applications of Cationic Aza-Cope Rearrangements*. For a brief review, see: Overman, L. E.; Ricca, D. J. In *Comprehensive Organic Synthesis*; Trost, B. M., Fleming, I., Heathcock, C. H., Eds.; Pergamon: Oxford, in press.

(2) See, inter alia: (a) Overman, L. E.; Mendelson, L.; Jacobsen, E. J. *J. Am. Chem. Soc.* **1983**, *105*, 6629. (b) Overman, L. E.; Jacobsen, E. J.; Doedens, R. J. *J. Org. Chem.* **1983**, *48*, 3393. (c) Overman, L. E.; Okazaki, M. E.; Jacobsen, E. J. *J. Org. Chem.* **1985**, *50*, 2403.

(3) Overman, L. E.; Kakimoto, M.-a.; Okazaki, M. E.; Meier, G. *J. Am. Chem. Soc.* **1983**, *105*, 6622. Overman, L. E.; Kakimoto, M.-a. *J. Am. Chem. Soc.* 1979, *101*, 1310.

(4) Overman, L. E.; Fukaya, C. *J. Am. Chem. Soc.* **1980**, *102*, 1454.

(5) Overman, L. E.; Sugai, S. *Helv. Chim. Acta* **1985**, *68*, 745.

0002-7863/91/1513-2598$02.50/0